

Enediyne Polyketide Synthases Stereoselectively Reduce the β -Ketoacyl Intermediates

to β -D-Hydroxyacyl Intermediates in Enediyne Core Biosynthesis

Hui-Ming Ge,[†] Tingting Huang,[†] Jeffrey D. Rudolf,[†] Jeremy R. Lohman,[†] Sheng-Xiong Huang,[†] Xun Guo,[†] and Ben Shen^{*,†,‡,§}

[†]Department of Chemistry, [‡]Department of Molecular Therapeutics, and [§]Natural Products Library Initiatives, The Scripps Research Institute, Jupiter, Florida 33458, United States

Supporting Information

Table of contents

General experimental procedures	S2
Cloning of <i>pksE</i> -KRs	S2
Overproduction of PKSE-KRs in <i>E. coli</i>	S3
Purification of PKSE-KRs	S3
Enzymatic activity of PKSE-KRs and chiral HPLC analysis	S3
Kinetic studies of PKSE-KRs	S3
Chemical synthesis of substrates and products	S4
General procedures for the preparation of MTPA esters	S8
Supplementary references	S9
Table S1. PCR primers used in this study	S10
Figure S1. The seven selected enediynes and their PKSEs	S11
Figure S2. Sequence comparison of KRs between selected type I PKSs and PKSEs	S13
Figure S3. SDS-PAGE of the purified KRs	S14
Figure S4, S5. ¹ H (400 MHz) and ¹³ C NMR (100 MHz) spectra of 1 in CDCl ₃	S15, 16
Figure S6, S7. ¹ H (400 MHz) and ¹³ C NMR (100 MHz) spectra of 2 in CDCl ₃	S17, 18
Figure S8, S9. ¹ H (400 MHz) and ¹³ C NMR (100 MHz) spectra of 3 in CDCl ₃	S19, 20
Figure S10, S11. ¹ H (400 MHz) and ¹³ C NMR (100 MHz) spectra of 4 or 7 in CDCl ₃	S21, 22
Figure S12, S13. ¹ H (400 MHz) and ¹³ C NMR (100 MHz) spectra of 5 or 8 in CDCl ₃	S23, 24
Figure S14, S15. ¹ H (400 MHz) and ¹³ C NMR (100 MHz) spectra of 6 or 9 in CDCl ₃	S25, 26
Figure S16, S17. ¹ H NMR (400 MHz) spectra of <i>S</i> -MTPA-5 and <i>R</i> -MTPA-5 in CDCl ₃	S27, 28
Figure S18. $\Delta\delta_{S-R}$ values (ppm) of MTPA esters of 5	S28
Figure S19, S20. ¹ H NMR (400 MHz) spectra of <i>S</i> -MTPA-6 and <i>R</i> -MTPA-6 in CDCl ₃	S29, 30
Figure S21. $\Delta\delta_{S-R}$ values (ppm) of MTPA esters of 6	S30
Figure S22. Enzymatic assay by following at 340 nm change as exemplified by SgcE-KR	S31
Figure S23. Pseudo-first order kinetic characterization of PKSE-KRs with 1 , 2 , and 3	S32

General experimental procedures

DNA oligonucleotide primers were synthesized by Integrated DNA Technologies. DNA sequencing was performed by Genewiz, Inc. Restriction enzymes, T4 DNA ligase, dNTPs, T4 DNA polymerase, and Platinum Pfx DNA polymerase were purchased from commercial sources. PCR was performed with a BIO-RAD S1000 Thermal cycler. DNA gel extraction and plasmid isolation were performed on Omega E.Z.N.A. Gel Extraction Kit and Omega E.Z.N.A. Plasmid Mini Kit, respectively. ^1H and ^{13}C NMR data were recorded at 25 °C on a Bruker AM-400 instrument. Optical rotation values were measured with an AUTOPOL[®] IV automatic polarimeter using a quartz cell with 1 mL capacity and a 1 dm path length. UV absorbance was measured on a Nanodrop 2000 UV-Vis spectrometer. High resolution electrospray ionization mass spectrometry (HRESIMS) was carried out on an Agilent 6230 TOF-LC-MS. Chiral HPLC was carried out with an Agilent 1260 infinity system equipped with quaternary pumps, a ChiralCel OC-H column (5 μm , 4.6 \times 250 mm), and a diode array detector. Protein purification was conducted on Äkta FPLC equipped with a HisTrap HP column (GE Healthcare Life Sciences).

Cloning of *pksE*-KRs

The genes encoding the SgcE-KR, KedE-KR, MdpE-KR, NcsE-KR, and Cale8-KR domains were amplified by PCR from cosmids pBS1006,¹ pBS16004,² pBS10004,³ pBS5013,⁴ and pBS14009,⁵ respectively, and cloned into pBS3080⁶ using the ligation independent method. PCR was performed with Plantium Pfx polymerase from Invitrogen using the primers described in Table 1 (also see Figures 1 and 2 for structures of the enediynes and protein sequence comparison among the PKSEs and PKSE-KRs). Briefly, pBS3080 was first digested with BsmF1 and purified by gel electrophoresis. The linearized vector was treated with T4 DNA polymerase in the presence of dGTP at 20 °C for 30 min followed by heating at 75 °C for 20 min to denature the polymerase, affording overhangs with complimentary sequences to clone the PCR amplified *pksE*-KRs. Similarly, each of the PCR amplified *pksE*-KR fragments was purified by gel electrophoresis and treated with T4 DNA polymerase in the presence of dCTP at 20 °C for 30 min followed by heating at 75 °C. The linearized and T4 DNA polymerase treated pBS3080 vector and the PCR amplified and T4 DNA polymerase treated *pksE*-KR fragments were then mixed at room temperature, annealed on ice for 5 min, and transformed into *E. coli* DH5 α for ligation independent cloning to construct the KR expression plasmids pBS1134, pBS16014, pBS10019, pBS5053, and pBS14016, respectively. Finally, the above plasmids were isolated from *E. coli* DH5 α and confirmed by DNA sequencing, in which the KRs were produced as fusion proteins with N-terminal His₆-tags. The genes encoding the DynE8-KR and UcmE-KR were amplified by PCR from the chromosomal DNA of *Micromonospora chersina* ATCC53710 and *Streptomyces uncialis* DCA2648 strains, respectively, using the primers listed in Table 1. The purified PCR products were cloned into pET-28a digested with NdeI and EcoRI to yield pBS14017 and pBS18001.

Overproduction of PKSE-KRs in *E. coli*

The expression plasmids for each of the *pksE-KR* genes were transformed into *E. coli* BL21 (DE3) and the resultant recombinant strains were grown overnight in 50 mL of LB media containing 50 µg/mL kanamycin. A 10 mL aliquot of the overnight culture was used to inoculate 1 L of LB containing 50 µg/mL kanamycin, which was then incubated at 37 °C with shaking at 250 rpm. Once the OD₆₀₀ reached ~0.4, the temperature was reduced to 18 °C. After the cultures reached thermal equilibrium, gene expression was induced by the addition of isopropyl β-D-1-thiogalactopyranoside (IPTG) to 0.25 mM, and incubation continued for an additional 18 hrs at 18 °C. *E. coli* cells were harvested by centrifugation at 3500 x g at 4 °C for 20 min.

Purification of PKSE-KRs

The *E. coli* cell pellets were resuspended in lysis buffer (50 mM Tris-HCl, pH 8.0, containing 1 µg/mL DNase, 300 mM NaCl, 10 mM imidazole, and 5% glycerol), sonicated (30 × 2 s on ice), and clarified by centrifugation at 15,000 rpm at 4 °C for 30 min. The supernatant was applied to a 5 mL HisTrap HP column and washed with lysis buffer. The column was washed with wash buffer (50 mM Tris-HCl, pH 8.0, containing 300 mM NaCl and 20 mM imidazole) and the PksE-KRs were eluted with wash buffer containing 250 mM imidazole. The purified protein was desalted through a PD-10 desalting column and concentrated with a Vivaspin ultrafiltration device (30,000 molecular weight cut-off). The purity of purified protein was assessed by 12% SDS-PAGE (Fig. S3), and the concentration was determined from the absorbance at 280 nm using the molar absorptivity of each protein calculated by ProtParam (<http://web.expasy.org/protparam/>).

Enzymatic activity of PKSE-KRs and chiral HPLC analysis

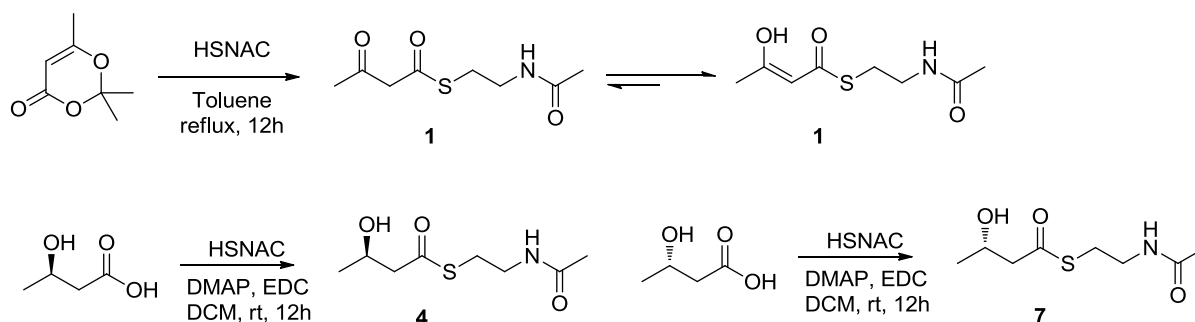
Each KR (10 µM) was incubated with 5 mM NADPH and 1 mM substrate in a total of 0.5 mL sodium phosphate buffer (100 mM, pH 7.2) at 28 °C for 3 h. The reaction product was extracted using ethyl acetate (3 × 400 µL), and after removal of the solvent, were resuspended in 500 µL of isopropanol. The isopropanol solution was separated using a ChiralCel OC-H column (250 × 4.6 mm) detected by 230 nm on an Agilent 1260 HPLC system. Compounds were eluted at 1 mL/min in 15% isopropanol in *n*-hexane.

Kinetic studies of PKSE-KRs

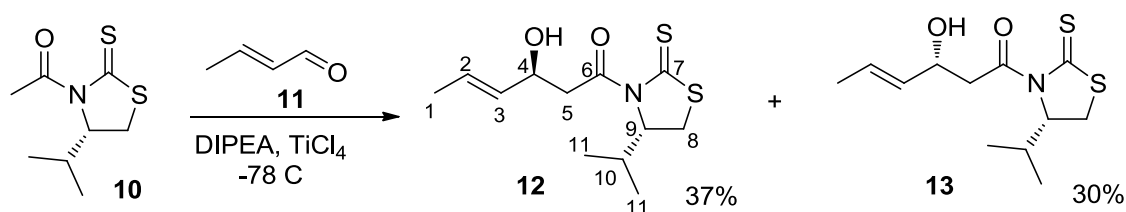
Kinetics studies for each KR were conducted spectrophotometrically by monitoring the change in absorbance at 340 nm, due to the consumption of NADPH ($\epsilon_{340} = 6220 \text{ M}^{-1} \text{ cm}^{-1}$). Assays were performed in the presence of 100 mM sodium phosphate buffer (pH 7.2), 10 µM KR, 0.3 mM NADPH, and varying concentration of substrates (0.05 – 2 mM) in a total

volume of 0.2 mL. Reactions were initiated by the addition of enzyme and read every 10 s. The approximation of k_{cat}/K_m values were calculated from three substrate concentrations using the limiting case of the Michaelis-Menten equation $v = (k_{cat}/K_m)[S][E]$ for low substrate concentrations ($[S] \ll K_m$).⁷ Each reaction was performed in triplicate and averaged (Figures 22 and 23).

Chemical synthesis of substrates and products



The known compounds **1**, **4** and **7** were synthesized following literature procedures.^{8,9} All spectroscopic data and physical properties matched those previously reported (Figures 4, 5, 10, and 11).^{8,9}

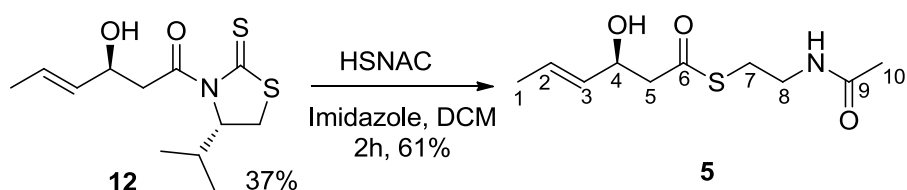


To a stirred solution of **10** (1 g, 4.9 mmol) in dry DCM (30 mL), TiCl₄ (1.0 M in DCM, 5.4 mL, 5.4 mmol) was added at 0 °C under argon. The reaction mixture was stirred for 5 min and then cooled to -78 °C. A solution of DIPEA (941 μL, 5.4 mmol) in DCM was added. The reaction mixture was stirred at -78 °C for 2 h. A solution of aldehyde **11** (700 mg, 10 mmol) was added to the reaction mixture, which was then stirred for 3 h at -78 °C. The reaction was quenched with 10 mL of saturated ammonium chloride. The layers were separated and the aqueous layer was extracted with DCM (3 × 20 mL). The combined organic layers were washed with brine (20 mL) and dried over Na₂SO₄. The solvent was removed *in vacuo* and the residue was purified using flash column chromatography (EtOAc/hexanes 1:5) to give diastereomers **12** (510 mg, 37% yield) and **13** (416 mg, 30% yield) as yellow oils.

Spectroscopic data for **12**. $[\alpha]_D^{25} = +446$ ($c = 0.65$, DCM), ¹H NMR (400 MHz, CDCl₃) δ 5.73 (m, 1H, H-3); 5.57 (m, 1H, H-2), 5.18 (m, 1H, H-9), 4.52 (m, 1H, H-4), 3.59 (dd, 1H, $J = 17.4, 9.0$ Hz, H-5), 3.52 (dd, 1H, $J = 11.5, 8.0$ Hz, H-8), 3.36 (dd, 1H, $J = 17.4, 3.2$ Hz,

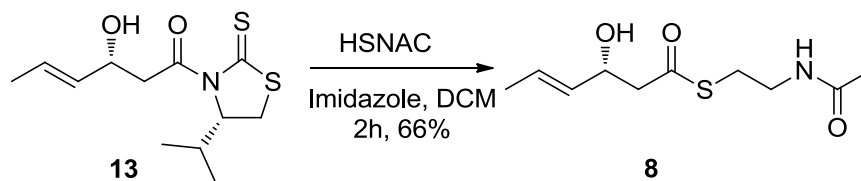
H-5), 3.04 (dd, 1H, $J = 11.5, 1.1$ Hz, H-8), 2.37 (m, 1H, H-10), 1.70 (ddd, 3H, $J = 6.4, 1.5, 0.9$ Hz, H-1), 1.06 (d, 3H, $J = 6.8$ Hz, H-11), 0.98 (d, 3H, $J = 6.8$ Hz, H-11); ^{13}C NMR (100 MHz, CDCl_3) δ 203.0, 173.1, 131.8, 127.4, 71.4, 69.1, 45.2, 30.8, 30.6, 19.1, 17.8, 17.7; HRESIMS for the $[\text{M} + \text{Na}]^+$ ion at m/z 296.0746 (calcd $[\text{M} + \text{Na}]^+$ ion for $\text{C}_{12}\text{H}_{19}\text{NO}_2\text{S}_2$ at m/z 296.0749).

Spectroscopic data for **13**. $[\alpha]_{\text{D}}^{25} = +487$ ($c = 0.55$, DCM), ^1H NMR (400 MHz, CDCl_3) δ 5.74 (m, 1H, H-3); 5.58 (m, 1H, H-2), 5.15 (m, 1H, H-9), 4.61 (m, 1H, H-4), 3.60 (dd, 1H, $J = 17.5, 9.0$ Hz, H-5), 3.53 (dd, 1H, $J = 11.3, 8.0$ Hz, H-8), 3.30 (dd, 1H, $J = 17.5, 3.2$ Hz, H-5), 3.02 (dd, 1H, $J = 11.3, 1.1$ Hz, H-8), 2.36 (m, 1H, H-10), 1.71 (ddd, 3H, $J = 6.2, 1.6, 0.9$ Hz, H-1), 1.07 (d, 3H, $J = 6.8$ Hz, H-11), 0.98 (d, 3H, $J = 6.8$ Hz, H-11); ^{13}C NMR (100 MHz, CDCl_3) δ 203.0, 172.6, 131.8, 127.3, 71.4, 68.8, 45.4, 30.8, 30.7, 19.1, 17.8, 17.7; HRESIMS m/z 296.0745 $[\text{M} + \text{Na}]^+$ (calcd $[\text{M} + \text{Na}]^+$ ion for $\text{C}_{12}\text{H}_{19}\text{NO}_2\text{S}_2$ at m/z 296.0749).

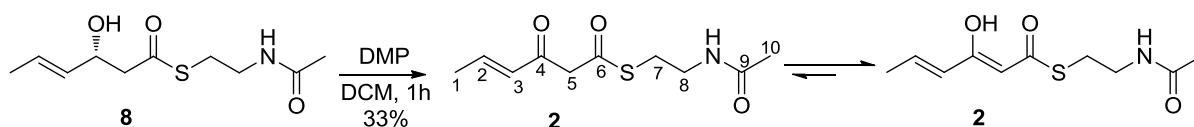


5: To a stirred solution of **12** (250 mg, 0.92 mmol) in 5 mL DCM, imidazole (188 mg, 2.76 mmol) and *N*-acetylcysteamine (219 mg, 1.84 mmol) were added. The reaction mixture was stirred until the yellow color disappeared. The reaction was quenched with 5 mL of saturated ammonium chloride. The organic layer was removed and the aqueous layer was extracted with DCM (3×10 mL). The combined organic layers were washed with brine and dried over Na_2SO_4 . The solvent was removed *in vacuo* and the residue was purified using flash column chromatography (DCM/MeOH 100:5) to give **5** (129 mg, 61%) as a white solid.

Spectroscopic data for **5**. $[\alpha]_{\text{D}}^{25} = -18.6$ ($c = 0.44$, DCM), ^1H NMR (400 MHz, CDCl_3) δ 5.90 (br s, 1H, NH), 5.74 (m, 1H, H-3); 5.50 (m, 1H, H-2), 4.54 (m, 1H, H-4), 3.44 (m, 2H, H-8), 3.05 (m, 2H, H-7), 2.78 (m, 2H, H-5), 2.60 (br s, 1H, OH), 1.97 (s, 3H, H-10), 1.70 (ddd, 3H, $J = 6.5, 1.6, 0.8$ Hz); ^{13}C NMR (100 MHz, CDCl_3) δ 198.8, 170.5, 131.6, 127.9, 69.6, 51.0, 39.3, 28.8, 23.2, 17.7; HRESIMS for the $[\text{M} + \text{Na}]^+$ ion at m/z 254.0822 (calcd $[\text{M} + \text{Na}]^+$ ion for $\text{C}_{10}\text{H}_{17}\text{NO}_3\text{S}$ at m/z 254.0821) (Figures 12 and 13).

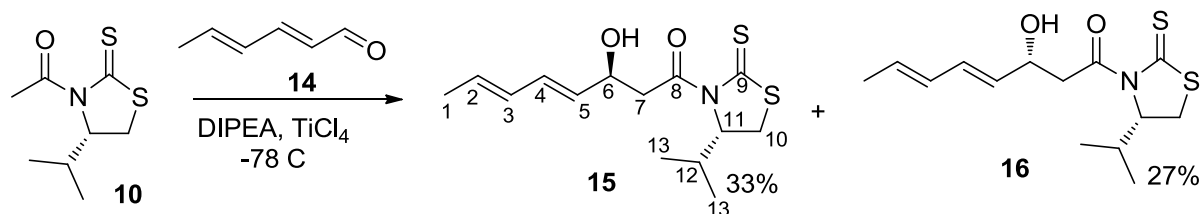


Compound **8** (112 mg, 66%) was synthesized from **13** using the method described above. **8**, 51 mg, white solid. NMR and MS data were identical to those of **5**. $[\alpha]_{\text{D}}^{25} = +16.7$ ($c = 0.42$, DCM) (Figures 12 and 13).



To a stirred solution of **8** (204 mg, 0.88 mmol) in 15 mL DCM, Dess-Martin periodinane (448 mg, 1.06 mmol) was added. The resulting solution was stirred at room temperature for 2 h. The reaction was quenched with 1 mL of isopropanol. The solution was washed with brine and dried with Na_2SO_4 . The solvent was removed *in vacuo* and the residue was purified using flash column chromatography (DCM/MeOH 100:2) to give **2** (keto:enol = 5:7, 66 mg, 33%) as a white solid.

Spectroscopic data for **2**. ^1H NMR (400 MHz, CDCl_3) δ 12.33 (br s, 1.4 H, enol-OH), 6.95 (m, 1H, keto-H-2); 6.77 (m, 1.4 H, enol-H-2), 6.20 (dq, 1H, $J = 15.4, 1.8\text{ Hz}$, keto-H-3), 5.99 (br s, 2.4H, NH), 5.75 (dq, 1.4H, $J = 1.2\text{ Hz}$, enol-H-3H-7), 5.43 (s, 1.4H, enol-H-5), 3.83 (s, 2H, keto-H-5), 3.47 (m, 4.8H, H-8), 3.10 (m, 4.8H, H-7), 1.97 (s, 7.2H, H-10), 1.96 (dd, 3H, $J = 1.6, 7.0\text{ Hz}$, keto-H-1), 1.90 (dd, 4.2H, $J = 1.6, 7.0\text{ Hz}$, keto-H-1); ^{13}C NMR (100 MHz, CDCl_3) δ 194.5, 192.7, 191.4, 170.4, 167.4, 146.2, 139.1, 131.1, 125.2, 99.5, 54.7, 40.0, 39.2, 29.3, 28.0, 23.2, 23.1, 18.5; HRESIMS for the $[\text{M} + \text{Na}]^+$ ion at m/z 252.0664 (calcd $[\text{M} + \text{Na}]^+$ ion for $\text{C}_{10}\text{H}_{15}\text{NO}_3\text{S}$ at m/z 252.0665) (Figures 6 and 7).

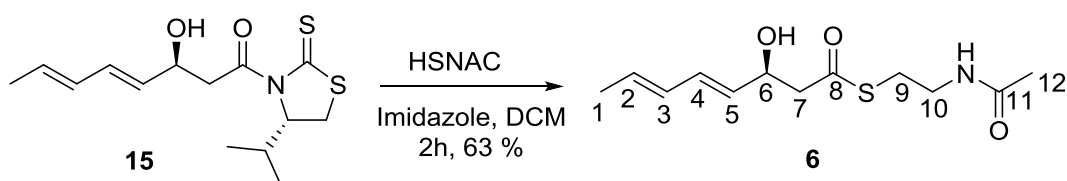


Compounds **15** (137 mg, 33%) and **16** (112 mg, 27%) were synthesized from (2*E*,4*E*)-hexa-2,4-dienal (**14**) using the method described for **12** and **13**.

Spectroscopic data for **15**. $[\alpha]_{\text{D}}^{25} = +282$ ($c = 0.63$), ^1H NMR (400 MHz, CDCl_3) δ 6.24 (dd, 1H, $J = 10.4, 15.6\text{ Hz}$, H-4); 6.04 (m, 1H, H-3), 5.74 (m, 1H, H-2), 5.61 (dd, 1H, $J = 6.2, 15.2\text{ Hz}$, H-5), 5.15 (m, 1H, H-11), 4.70 (m, 1H, H-6), 3.61 (dd, 1H, $J = 17.4, 9.0\text{ Hz}$, H-7), 3.52 (dd, 1H, $J = 11.3, 8.0\text{ Hz}$, H-10), 3.32 (dd, 1H, $J = 17.4, 3.2\text{ Hz}$, H-7), 3.03 (dd, 1H, $J = 11.3, 1.1\text{ Hz}$, H-10), 2.37 (m, 1H, H-12), 1.75 (dd, 3H, $J = 6.2, 1.1\text{ Hz}$, H-1), 1.07 (d, 3H, $J = 6.8\text{ Hz}$, H-13), 0.98 (d, 3H, $J = 6.8\text{ Hz}$, H-13); ^{13}C NMR (100 MHz, CDCl_3) δ 203.0, 172.4, 131.1, 130.7, 130.6, 130.5, , 127.3, 71.4, 68.5, 45.4, 30.8, 30.7, 19.1, 18.1, 17.8; HRESIMS

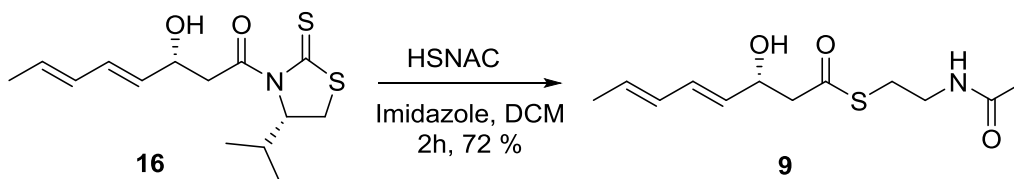
for the $[M + Na]^+$ ion at m/z 322.0901 (calcd $[M + Na]^+$ ion for $C_{14}H_{21}NO_2S_2$ at m/z 322.0906).

Spectroscopic data for **16**. $[\alpha]_D^{25} = +291$ ($c = 0.51$, DCM), 1H NMR (400 MHz, $CDCl_3$) δ 6.25 (dd, 1H, $J = 10.4, 15.6$ Hz, H-4); 6.04 (m, 1H, H-3), 5.74 (m, 1H, H-2), 5.59 (dd, 1H, $J = 6.2, 15.2$ Hz, H-5) 5.17 (m, 1H, H-11), 4.61 (m, 1H, H-6), 3.62 (dd, 1H, $J = 17.0, 9.0$ Hz, H-7), 3.53 (dd, 1H, $J = 11.5, 8.0$ Hz, H-10), 3.38 (dd, 1H, $J = 17.0, 3.2$ Hz, H-7), 3.04 (dd, 1H, $J = 11.5, 1.0$ Hz, H-10), 2.37 (m, 1H, H-12), 1.75 (dd, 3H, $J = 6.7, 1.2$ Hz, H-1), 1.07 (d, 3H, $J = 6.8$ Hz, H-13), 0.98 (d, 3H, $J = 6.9$ Hz, H-13); ^{13}C NMR (100 MHz, $CDCl_3$) δ 203.0, 172.8, 131.3, 130.7, 130.6, 130.3, 71.3, 69.0, 45.1, 30.7, 30.6, 19.1, 18.1, 17.8; HRESIMS for the $[M + Na]^+$ ion at m/z 322.0910 (calcd $[M + Na]^+$ ion for $C_{14}H_{21}NO_2S_2$ at m/z 322.0906).



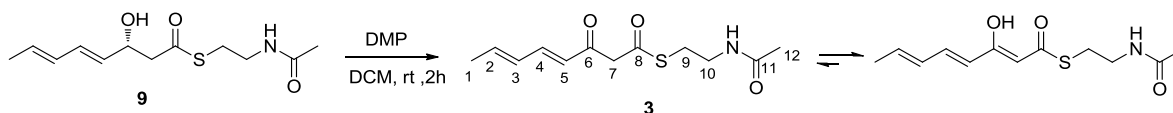
Compound **6** (133mg, 63%) was synthesized from **15** using the method described for **5**.

Spectroscopic data for **6**. $[\alpha]_D^{25} = -11.6$ ($c = 0.29$, DCM), 1H NMR (400 MHz, $CDCl_3$) δ 6.24 (dd, 1H, $J = 10.4, 14.4$ Hz, H-4), 6.03 (m, 1H, H-3), 5.85 (br s, 1H, NH), 5.74 (m, 1H, H-2); 5.55 (dd, 1H, $J = 5.7, 14.8$ Hz, H-5), 4.62 (m, 1H, H-6), 3.45 (m, 2H, H-10), 3.05 (m, 2H, H-9), 2.81 (m, 2H, H-7), 2.60 (br s, 1H, OH), 1.96 (s, 3H, H-12), 1.75 (dd, 3H, $J = 6.5, 1.2$ Hz) ^{13}C NMR (100 MHz, $CDCl_3$) δ 198.5, 170.7, 131.5, 131.0, 130.43, 130.41, 69.3, 51.1, 39.3, 28.8, 23.2, 18.1; HRESIMS for the $[M + Na]^+$ ion at m/z 280.0972 (calcd $[M + Na]^+$ ion for $C_{12}H_{19}NO_3S$ at m/z 280.0978) (Figure 14 and 15).



Compound **9** (77mg, 72%) was synthesized from **16** using the method described for **5**.

Spectroscopic data for **9**. $[\alpha]_D^{25} = +13.0$ ($c = 0.27$, DCM), the NMR and MS data were identical to those of **6** (Figures 14 and 15).



Compound **3** was synthesized from **9** using the method described for synthesizing **2**.

3: 37 mg, white solid, yield 33%. ^1H NMR (400 MHz, CDCl_3) δ 12.26 (br s, 0.75 H, OH), 7.04-7.15 (m, overlapped, 1H, H-4), 6.03-6.20 (m, overlapped, 2.25H, H-3), 5.89 (br s, 1H, NH), 5.64 (d, $J = 15.2$ Hz, 0.75H, enol-H-5); 5.41 (s, 0.75 H, enol-H-7), 3.78 (s, 0.5 H, keto-H-7), 3.41 (m, 2H, H-10), 3.03 (m, 2H, H-9) 1.90 (s, 3H, H-12), 1.83 (d, 0.75 H, $J = 6.5$ Hz), 1.79 (d, 2.25 H, $J = 6.5$ Hz) ^{13}C NMR (100 MHz, CDCl_3) δ 194.1, 192.7, 191.6, 170.5, 170.4, 167.9, 145.8, 142.7, 140.1, 138.2, 130.6, 130.1, 128.2, 126.4, 124.2, 122.0, 100.5, 55.3, 40.0, 39.3, 29.7, 29.3, 28.0, 23.2, 23.1, 19.0, 18.8; HRESIMS for the $[\text{M} + \text{Na}]^+$ ion at m/z 278.0820 (calcd $[\text{M} + \text{Na}]^+$ ion for $\text{C}_{12}\text{H}_{17}\text{NO}_3\text{S}$ at m/z 278.0821) (Figures 8 and 9).

General procedures for the preparation of MTPA esters

(*R*)- or (*S*)-MTPA chloride (4-fold mM excess over starting alcohol) was added to a solution of starting alcohol (2 mg) in pyridine (200 μL), and the resulting mixture was allowed to stand at room temperature for 4 h. The mixture was quenched with 10 μl of water and stirred for an additional 10 min, then diluted with DCM (5 mL). The solvent was removed on a rotary evaporator. The crude product was purified by the preparative TLC (DCM / MeOH = 20:1) to give the MTPA ester. The $\Delta\delta_{\text{S-R}}$ values (ppm) of MTPA esters for compound **5** and **6** see Fig. S18 and S21, respectively.

Spectroscopic data for (*S*)-MTPA-**5**. ^1H NMR (400 MHz, CDCl_3) δ 7.38-7.49 (m, 5H, phenyl protons at MTPA), 5.95 (m, 1H, H-3), 5.88 (m, 1H, H-4), 5.78 (br s, 1H, NH), 5.50 (m, 1H, H-2); 3.51 (br s, 3H, OMe in MTPA), 3.35 (m, 2H, H-8), 3.03 (m, 1H, H-5a), 2.97 (m, 2H, H-7), 2.81 (m, 1H, H-5b), 1.95 (s, 3H, H-10), 1.73 (dd, 3H, $J = 6.5, 1.5$ Hz, H-1); HRESIMS for the $[\text{M} + \text{Na}]^+$ ion at m/z 470.1217 (calcd $[\text{M} + \text{Na}]^+$ ion for $\text{C}_{20}\text{H}_{24}\text{NF}_3\text{O}_5\text{S}$ at m/z 470.1220) (Figures 16 and 18).

Spectroscopic data for (*R*)-MTPA-**5**. ^1H NMR (400 MHz, CDCl_3) δ 7.38-7.49 (m, 5H, phenyl protons at MTPA), 5.87 (m, 1H, H-4); 5.86 (m, 1H, H-3), 5.81 (br s, 1H, NH), 5.39 (m, 1H, H-2), 3.51 (br s, 3H, OMe in MTPA), 3.39 (m, 2H, H-8), 3.07 (m, 1H, H-5a), 3.03 (m, 2H, H-7), 2.85 (m, 1H, H-5b), 1.94 (s, 3H, H-10), 1.69 (dd, 3H, $J = 6.6, 1.6$ Hz, H-1); HRESIMS for the $[\text{M} + \text{Na}]^+$ ion at m/z 470.1213 (calcd $[\text{M} + \text{Na}]^+$ ion for $\text{C}_{20}\text{H}_{24}\text{NF}_3\text{O}_5\text{S}$ at m/z 470.1220) (Figures 17 and 18).

Spectroscopic data for (*S*)-MTPA-**6**. ^1H NMR (400 MHz, CDCl_3) δ 7.32-7.40 (m, 5H, phenyl protons at MTPA), 6.29 (m, 1H, H-5), 5.94 (m, 1H, H-2), 5.87 (m, 1H, H-6), 5.75 (m, 1H, H-3), 5.72 (br s, 1H, NH), 5.45 (m, 1H, H-4), 3.45 (br s, 3H, OMe in MTPA), 3.29 (m, 2H, H-10), 2.98 (m, 1H, H-7a), 2.91 (m, 2H, H-9), 2.74 (m, 1H, H-7b), 1.88 (s, 3H, H-12), 1.72 (dd, 3H, H-1, $J = 6.6, 1.6$ Hz, H-1); HRESIMS for the $[\text{M} + \text{Na}]^+$ ion at m/z 496.1368 (calcd $[\text{M} + \text{Na}]^+$ ion for $\text{C}_{22}\text{H}_{26}\text{NF}_3\text{O}_5\text{S}$ at m/z 496.1376) (Figures 19 and 21).

Spectroscopic data for (**R**)-MTPA-6. ¹H NMR (400 MHz, CDCl₃) δ 7.32-7.40 (m, 5H, phenyl protons at MTPA), 6.20 (m, 1H, H-5), 5.90 (m, 1H, H-2), 5.86 (m, 1H, H-6), 5.74 (br s, 1H, NH), 5.71 (m, 1H, H-3), 5.34 (m, 1H, H-4), 3.45 (br s, 3H, OMe in MTPA), 3.32 (m, 2H, H-10), 3.02 (m, 1H, H-7a), 2.96 (m, 2H, H-9), 2.78 (m, 1H, H-7b), 1.87 (s, 3H, H-12), 1.71 (dd, 3H, H-1, *J* = 6.5, 1.6 Hz, H-1); HRESIMS for the [M + Na]⁺ ion at *m/z* 496.1371 (calcd [M + Na]⁺ ion for C₂₂H₂₆NF₃O₅S at *m/z* 496.1376) (Figures 20 and 21).

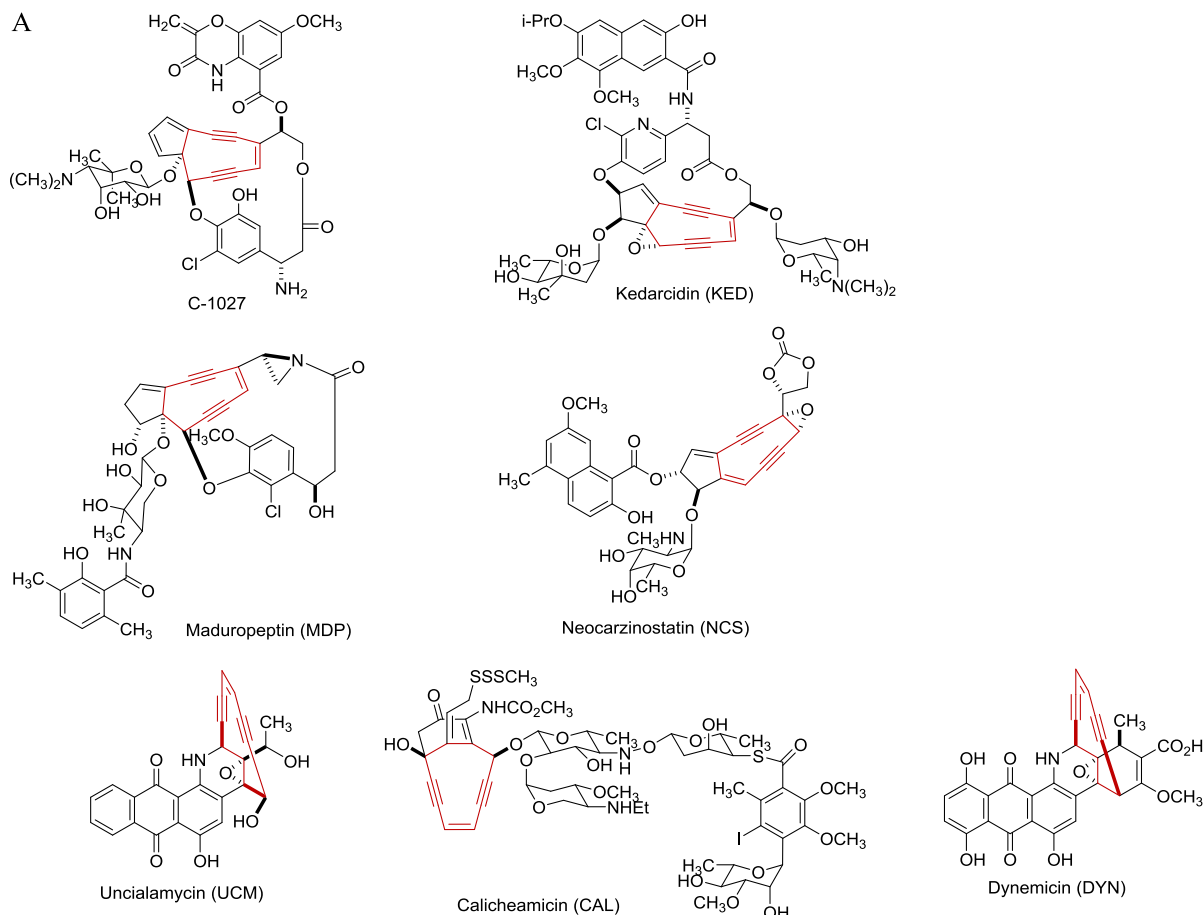
Supplementary references

1. Liu, W.; Christenson, S. D.; Standage, S.; Shen, B. *Science* **2002**, *297*, 1170-1173.
2. Lohman, J. R.; Huang, S. X.; Horsman, G. P.; Dilfer, P. E.; Huang, T.; Chen, Y.; Wendt-Pienkowski, E.; Shen, B. *Molecular. Biosystems* **2013**, *9*, 478-491.
3. Van Lanen, S. G.; Oh, T. J.; Liu, W.; Wendt-Pienkowski, E.; Shen, B. *J. Am. Chem. Soc.* **2007**, *129*, 13082-13094.
4. Liu, W.; Nonaka, K.; Nie, L.; Zhang, J.; Christenson, S. D.; Bae, J.; Van Lanen, S. G.; Zazopoulos, E.; Farnet, C. M.; Yang, C. F.; Shen, B. *Chem. Biol.* **2005**, *12*, 293-302.
5. Horsman, G. P.; Chen, Y. H.; Thorson, J. S.; Shen, B. *Proc. Natl. Acad. Sci. USA* **2010**, *107*, 11331-11335.
6. Huang, S. X.; Lohman, J. R.; Huang, T.; Shen, B. *Proc. Natl. Acad. Sci. USA* **2013**, *110*, 8069-8074.
7. Bonnett, S. A.; Whicher, J. R.; Papireddy, K.; Florova, G.; Smith, J. L.; Reynolds, K. A. *Chem. Biol.* **2013**, *20*, 772-783.
8. Gilbert, I. H.; Ginty, M.; O'Neill, J. A.; Simpson, T. J.; Staunton, J.; Willis, C. L. *Bioorg. Med. Chem. Lett.* **1995**, *5*, 1587-1590.
9. Gruschow, S.; Buchholz, T. J.; Seufert, W.; Dordick, J. S.; Sherman, D. H. *Chembiochem* **2007**, *8*, 863-868.

Table S1. Primers used in this study with the NdeI/EcoRI sites used for cloning underlined

Primer name	primer sequence ^a
SgcE-KR forward	5'-AAAACCTCTATTTCCAGTCGGGTGCGGACCCGACG-3'
SgcE-KR reverse	5'-TACTTACTTAAATGTTACCCGGTGAAACGCAGCAG-3'
KedE-KR forward	5'-AAAACCTCTATTTCCAGTCGGGGCGCGAGGAGGAG-3'
KedE-KR reverse	5'-TACTTACTTAAATGTTAGAACCGCTTCAGCGG-3'
MdpE-KR forward	5'-AAAACCTCTATTTCCAGTCGGCGGTGCGGGGGGCC-3'
MdpE-KR reverse	5'-TACTTACTTAAATGTTACCCGTGAACCGCAA-3'
NcsE-KR forward	5'-AAAACCTCTATTTCCAGTCGGCCGATGCCGGTGCG-3'
NcsE-KR reverse	5'-TACTTACTTAAATGTTAGCCGGTGAACCGGAG-3'
CalE8-KR forward	5'-AAAACCTCTATTTCCAGTCGGGGGTGCGCCCGTGG-3'
CalE8-KR reverse	5'-TACTTACTTAAATGTTAGGTGAAGCGCAGCAG-3'
DynE8-KR forward	5'-AGGCAATTCCATATGCCCCGCCGAGCTGCCC-3'
DynE8-KR reverse	5'-CCGGAATTCTCACTCCAGGAAACGGCCGTG-3'
UcmE-KR forward	5'-AGGCAATTCCATATGGCCGACGAGGCCCTCC-3'
UcmE-KR reverse	5'-CCGGAATTCTCACTCCGGAACCGTCCGTCC-3'

^aPrimers used to make the expression constructs for *sgcE-KR*, *kedE-KR*, *mdpE-KR*, *ncsE-KR*, and *calE8-KR* by the ligation independent cloning strategy. Primers used to make the expression constructs for *dynE8-KR* and *ucmE-KR* by direct cloning strategy with the NdeI/EcoRI sites underlined.



	SgcE	CalE8	DynE8	KedE	MdpE	NcsE	UcmE
SgcE	-	55	40	53	64	68	44
CalE8	55	-	43	55	58	54	46
DynE8	40	43	-	42	41	41	42
KedE	53	55	42	-	55	52	46
MdpE	64	58	41	55	-	62	44
NcsE	68	54	41	52	62	-	43
UcmE	44	46	42	46	44	43	-

Figure S1. The selected seven enediynes and their PKSEs. (A) Structures of four nine-membered (C-1027, KED, MDP, NCS) and three ten-membered enediynes (CAL, DYN, UCM) with their enediynes cores highlighted in red. (B) Domain organization of PKSEs and their sequence identities (%). The accession numbers for each of the PKSEs are: SgcE (AAL06699), CalE8 (AAM94794), DynE8 (AAN79725), KedE (AFV52145), MdpE (AAQ17110), NcsE (AAM77986), and UcmE (KM017987).

A

```

1019      1029      1039      1051      1061      1065      1175
SgcEKR      . . . . .
CalE8KR      . . . . .
DynE8KR      . . . . .
KedEKR      . . . . .
MdpEKR      . . . . .
NcsEKR      . . . . .
UcmEKR      . . . . .
Ty1KR6      . . . . .
Ty1KR18     . . . . .
Ty1KR1      . . . . .
EryKR1      . . . . .

1086      1096      1105      1115      1125      1135      1145      1151
SgcEKR      . . . . .
CalE8KR      . . . . .
DynE8KR      . . . . .
KedEKR      . . . . .
MdpEKR      . . . . .
NcsEKR      . . . . .
UcmEKR      . . . . .
Ty1KR6      . . . . .
Ty1KR18     . . . . .
Ty1KR1      . . . . .
EryKR1      . . . . .

1161      1170      1180      1190      1198      1208      1218      1227      1237      1247      1257
SgcEKR      . . . . .
CalE8KR      . . . . .
DynE8KR      . . . . .
KedEKR      . . . . .
MdpEKR      . . . . .
NcsEKR      . . . . .
UcmEKR      . . . . .
Ty1KR6      . . . . .
Ty1KR18     . . . . .
Ty1KR1      . . . . .
EryKR1      . . . . .

1267      1277      1287      1296      1306      1316      1326      1334      1344      1354      1364
SgcEKR      . . . . .
CalE8KR      . . . . .
DynE8KR      . . . . .
KedEKR      . . . . .
MdpEKR      . . . . .
NcsEKR      . . . . .
UcmEKR      . . . . .
Ty1KR6      . . . . .
Ty1KR18     . . . . .
Ty1KR1      . . . . .
EryKR1      . . . . .

1374      1384      1394      1401      1411      1421      1431      1441      1451
SgcEKR      . . . . .
CalE8KR      . . . . .
DynE8KR      . . . . .
KedEKR      . . . . .
MdpEKR      . . . . .
NcsEKR      . . . . .
UcmEKR      . . . . .
Ty1KR6      . . . . .
Ty1KR18     . . . . .
Ty1KR1      . . . . .
EryKR1      . . . . .

```

Figure S2 continues to the next page

B

	SgcE-KR	CalE8-KR	DynE8-KR	KedE-KR	MdpE-KR	NcsE-KR	UcmE-KR
SgcE-KR	-	55	37	53	63	67	41
CalE8-KR	55	-	40	51	57	54	42
DynE8-KR	37	40	-	39	40	40	37
KedE-KR	53	51	39	-	53	52	46
MdpE-KR	63	57	40	53	-	61	41
NcsE-KR	67	54	40	52	61	-	41
UcmE-KR	41	42	38	46	41	41	-

Figure S2. Protein sequence comparison of KR domains between selected noniterative type I PKSs and PKSEs. (A) Protein sequence alignment of KR domains with the conserved KSY catalytic residues, NADPH binding site, and diagnostic LDD motif in B-type KRs and W residue in A-type KRs highlighted in green, yellow, and red, respectively. See Figure S1 legend for accession numbers of the seven PKSEs. (B) Sequence identities (%) of KR domains among the seven PKSEs. The accession numbers for the three A-type KRs are TylKR6 (AAB66508), AmphKR2 (AAK73513), and AmphKR1 (AAK73513). The accession numbers for the three B-type KRs are AmphKR18 (AAK73593), TylKR1 (AAB66504), and EryKR1 (AAV51820). The crystal structures for AmphKR2 (3JME), EryKR1 (2FR1), and TylKR1 (2Z5L) have been previously determined.

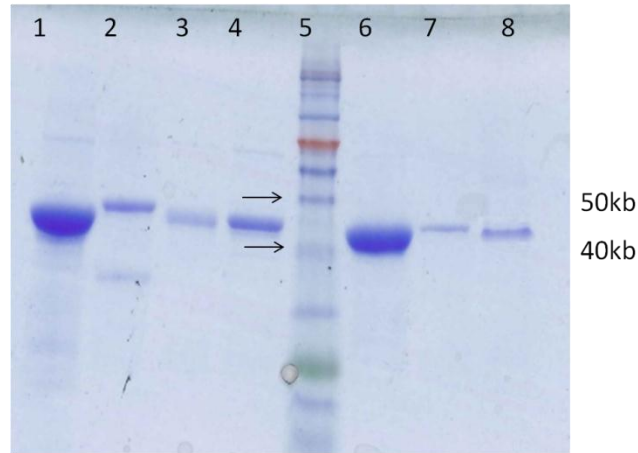


Figure S3. SDS-PAGE of the purified KR_s. Lane 1, SgcE-KR (47,878 Da); lane 2, KedE-KR (48,284 Da); lane 3, MdpE-KR (47,163 Da); lane 4, NcsE-KR (48,553 Da); lane 5, protein ladder; lane 6, CalE8-KR (46,590 Da); lane 7, UcmE-KR (48,054 Da); and lane 8, DynE8-KR (46,239 Da). Given in parentheses are calculated molecular weights for each of the recombinant proteins.

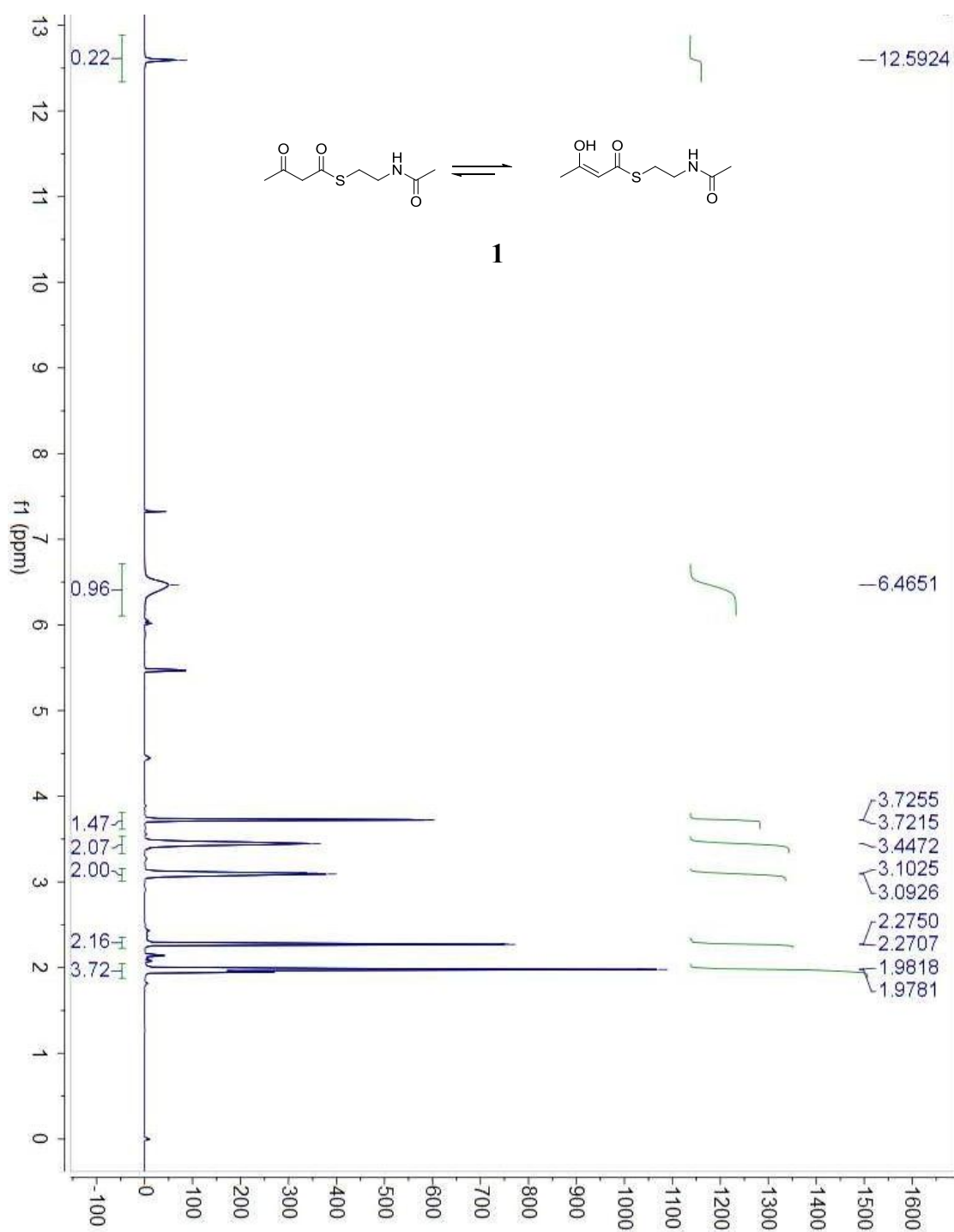


Figure S4. ^1H NMR (400 MHz) spectrum of compound **1** in CDCl_3

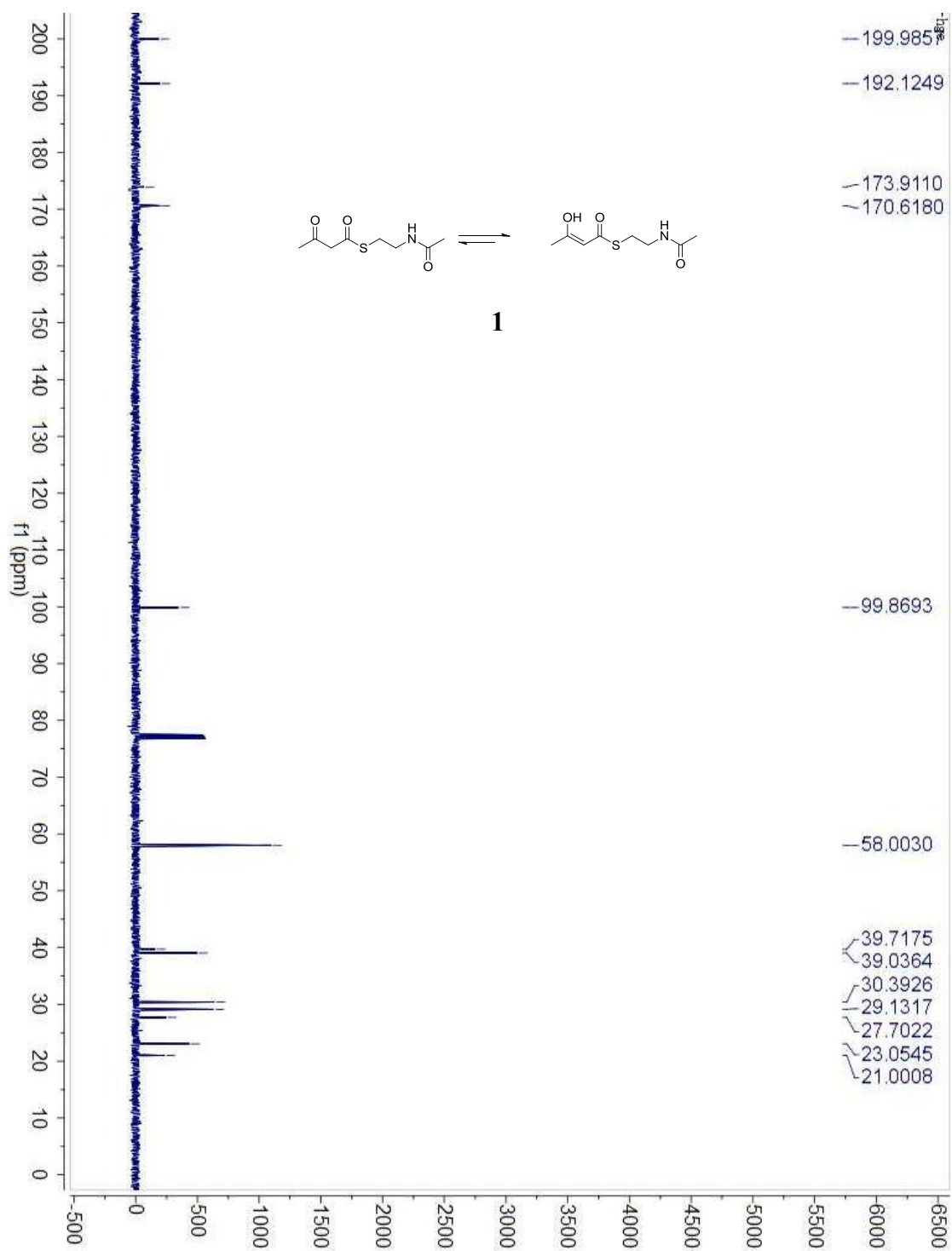


Figure S5. ¹³C NMR (100 MHz) spectrum of compound **1** in CDCl₃

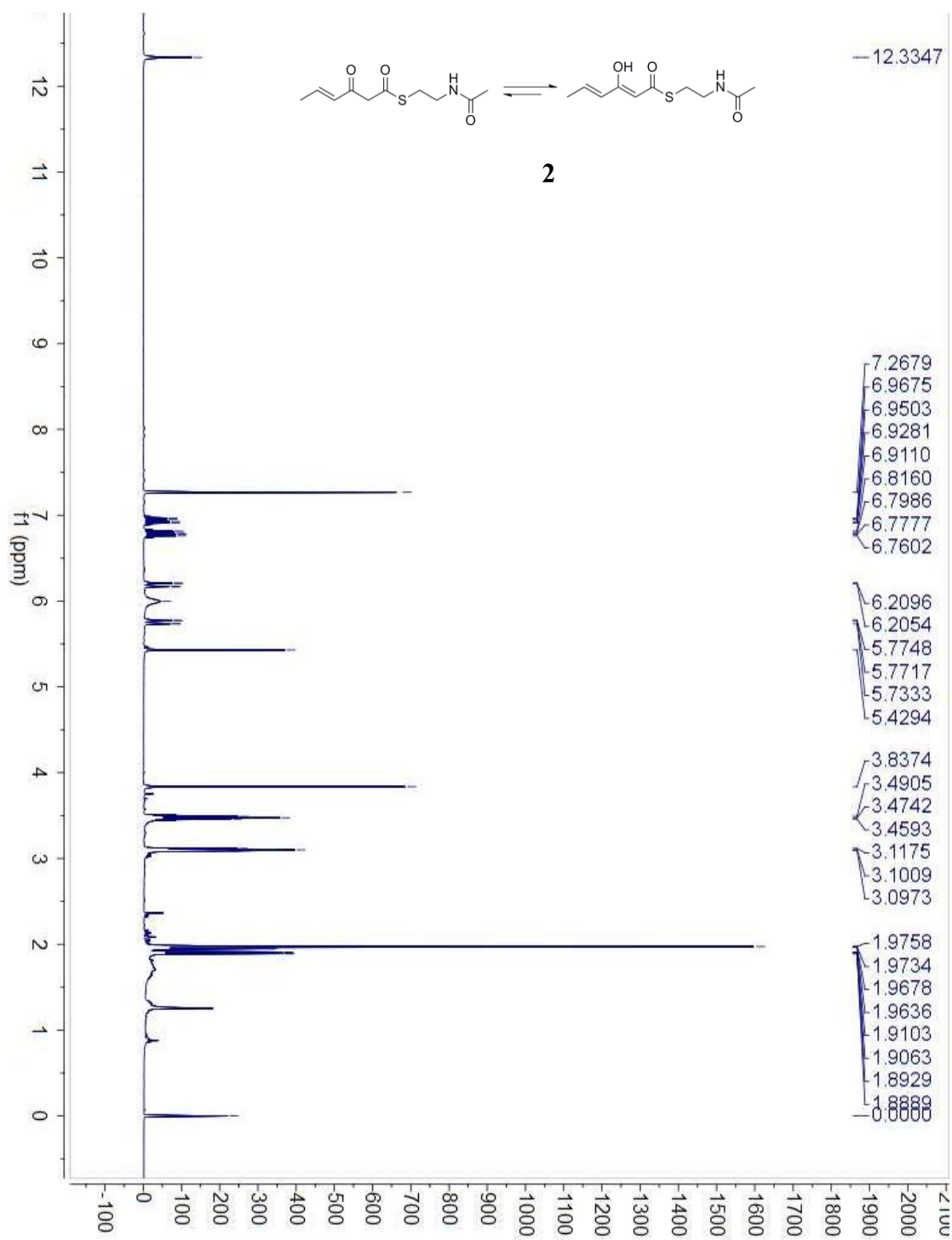


Figure S6. ^1H NMR (400 MHz) spectrum of compound **2** in CDCl_3

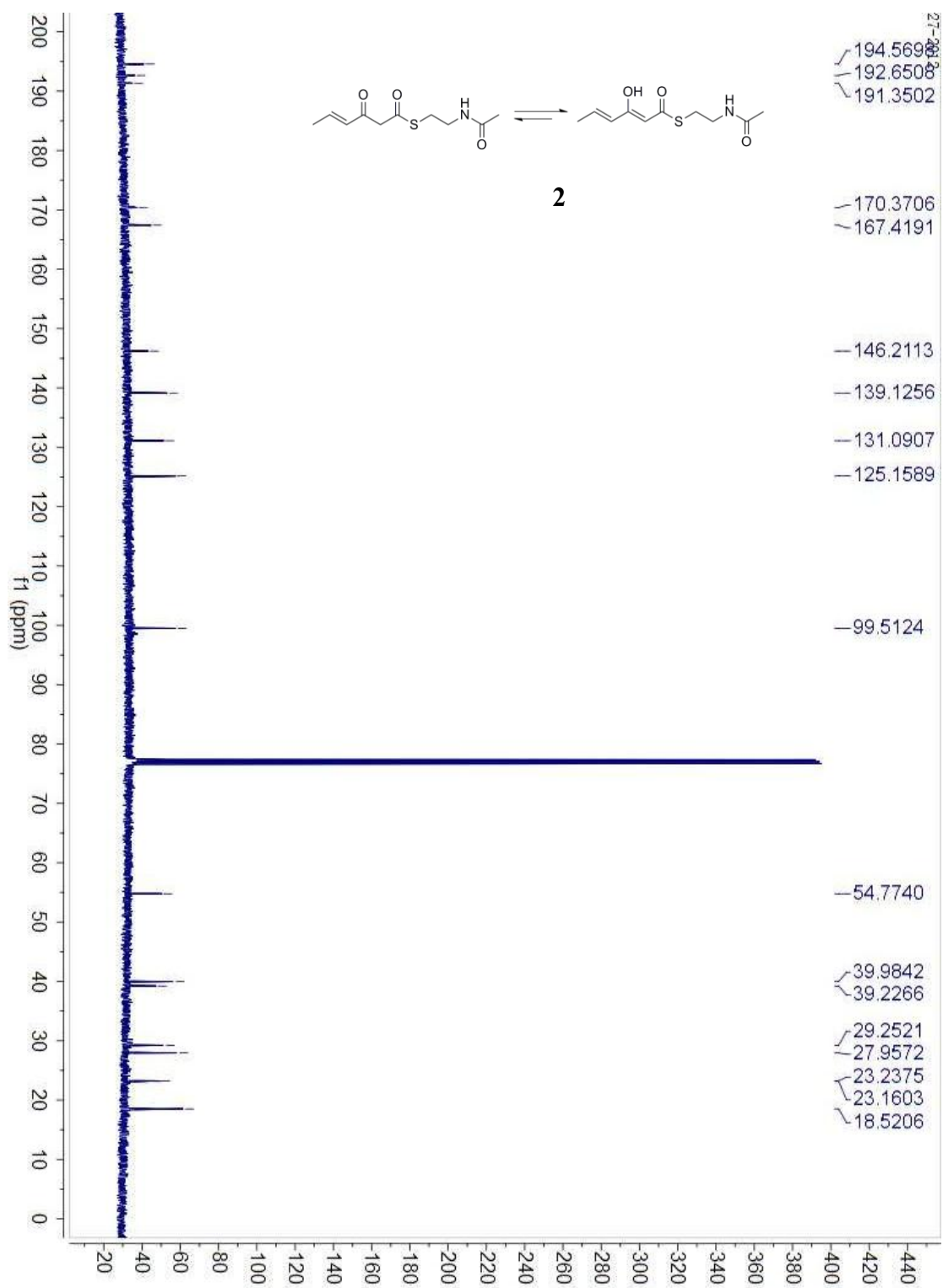


Figure S7. ¹³C NMR (100 MHz) spectrum of compound **2** in CDCl₃

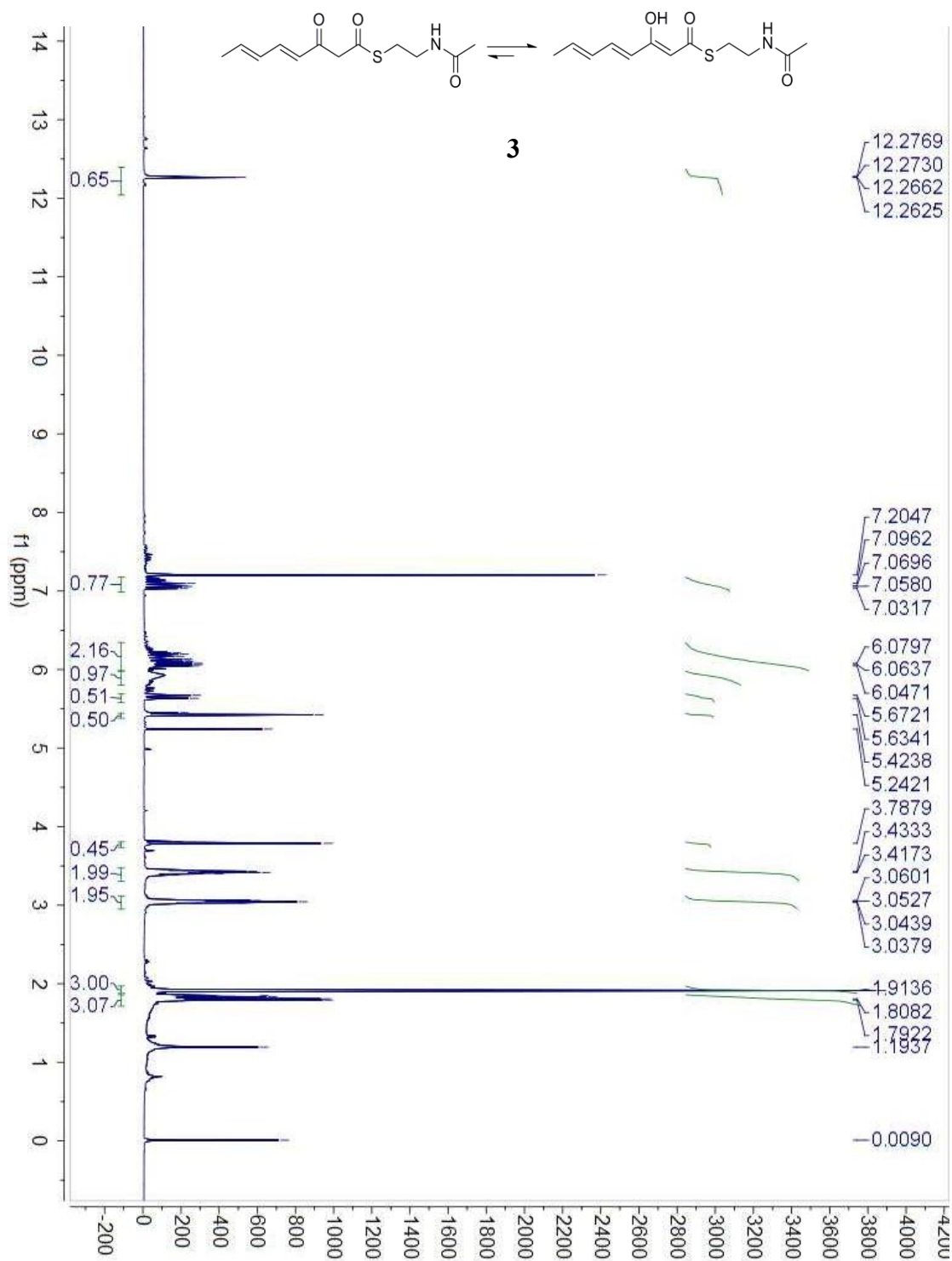


Figure S8. ^1H NMR (400 MHz) spectrum of compound **3** in CDCl_3

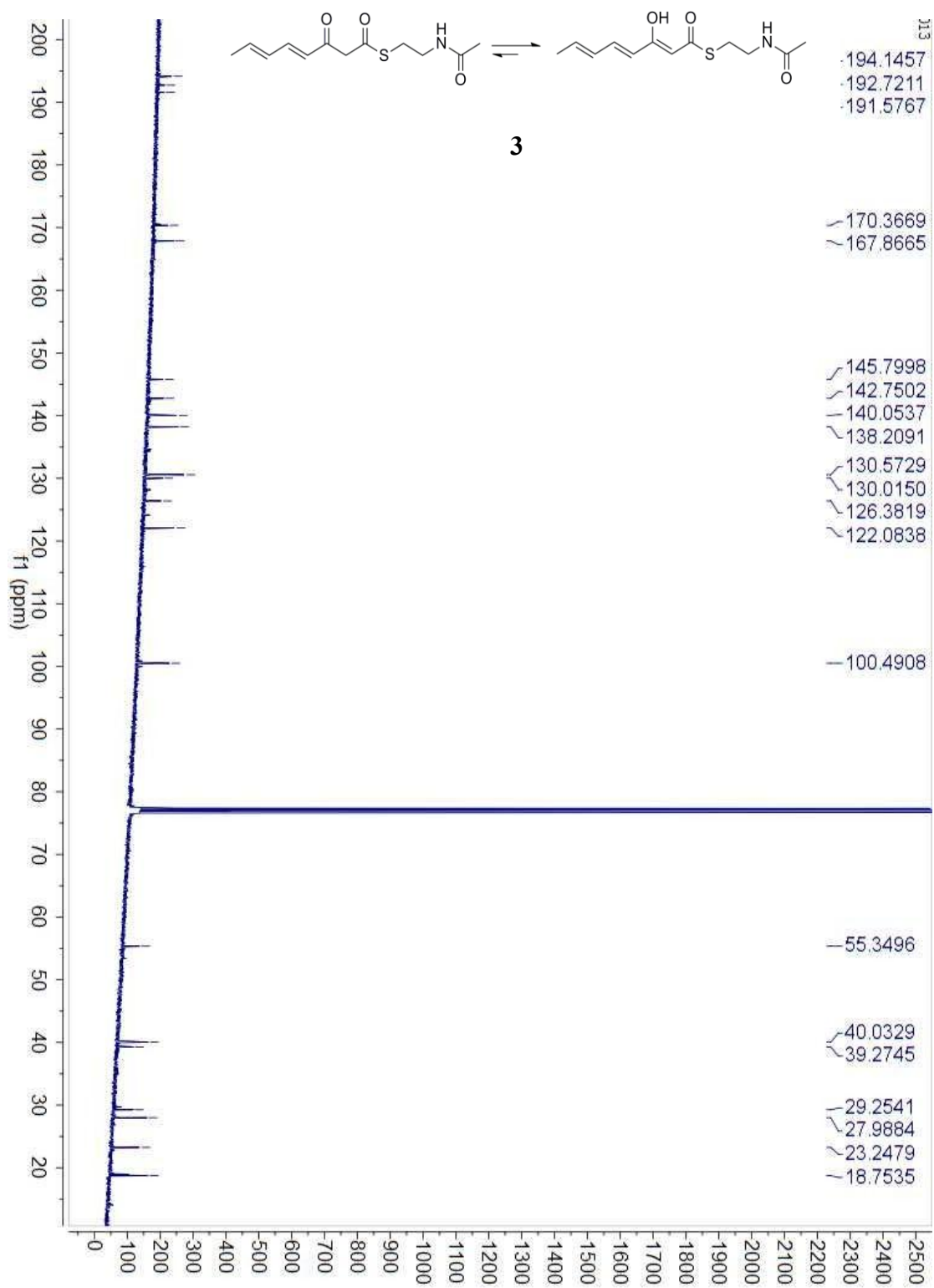


Figure S9. ¹³C NMR (100 MHz) spectrum of compound **3** in CDCl₃

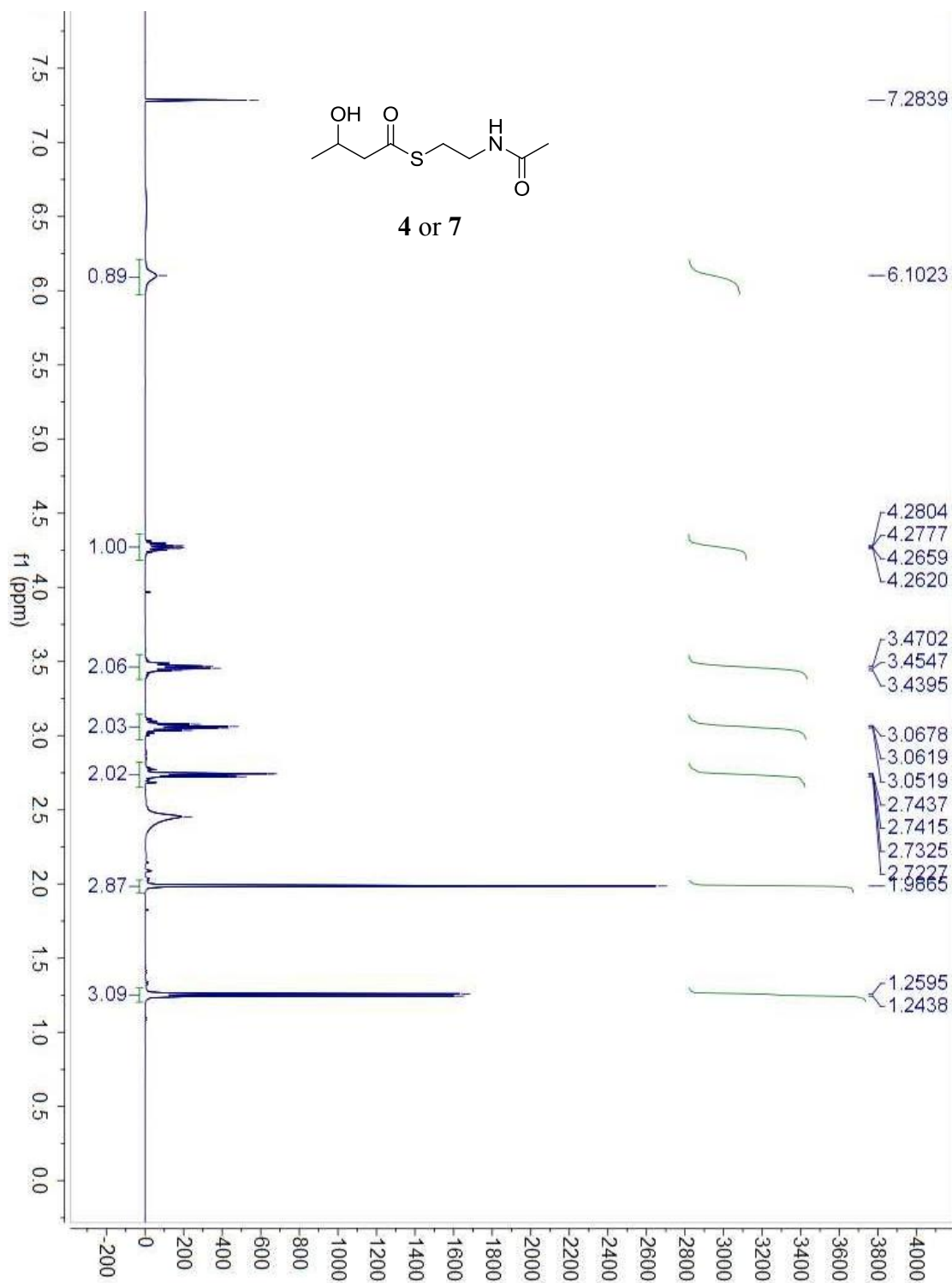


Figure S10. ^1H NMR (400 MHz) spectrum of compound **4** or **7** in CDCl_3

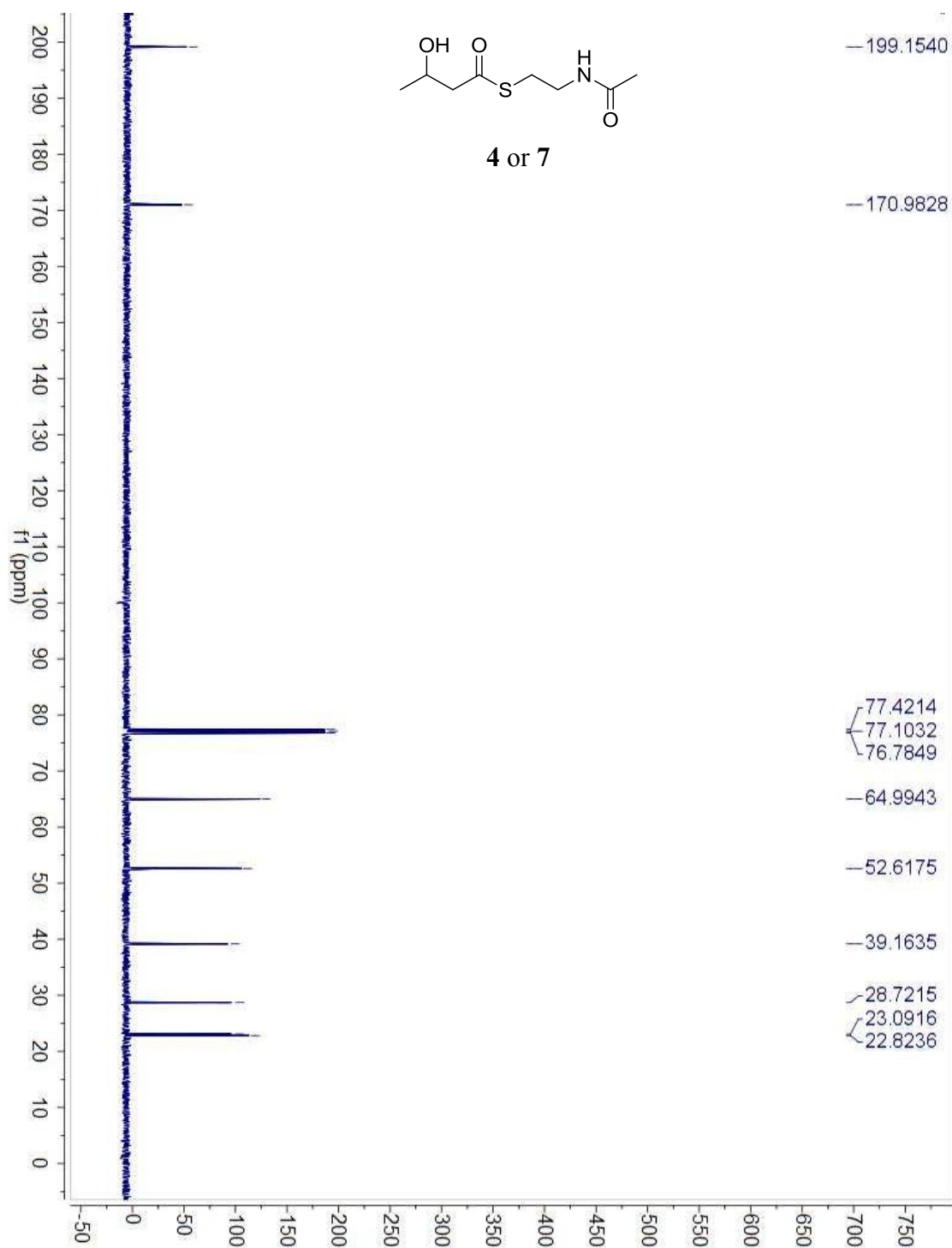


Figure S11. ^{13}C NMR (100 MHz) spectrum of compound 4 or 7 in CDCl_3

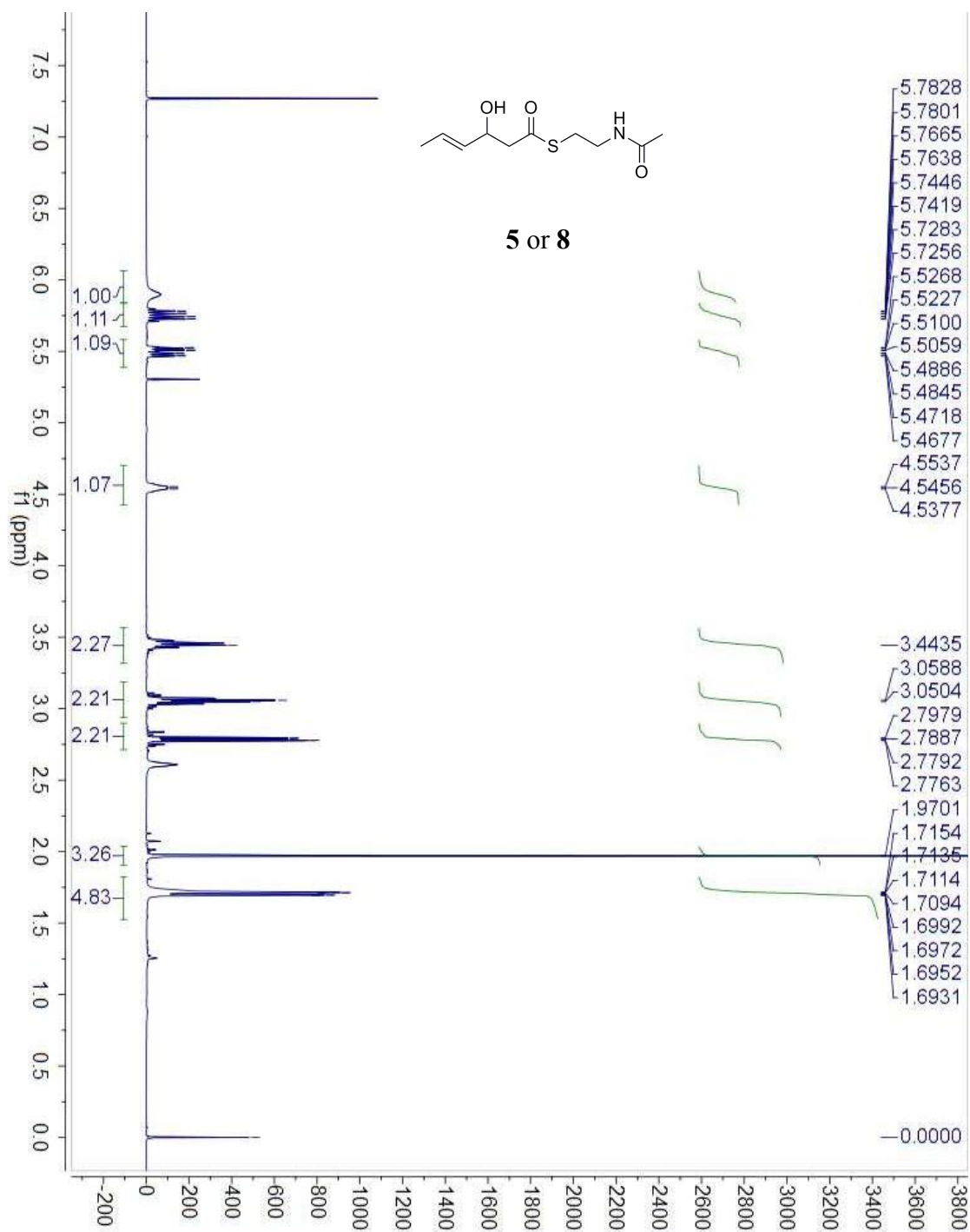


Figure S12. ^1H NMR (400 MHz) spectrum of compound **5 or 8** in CDCl_3

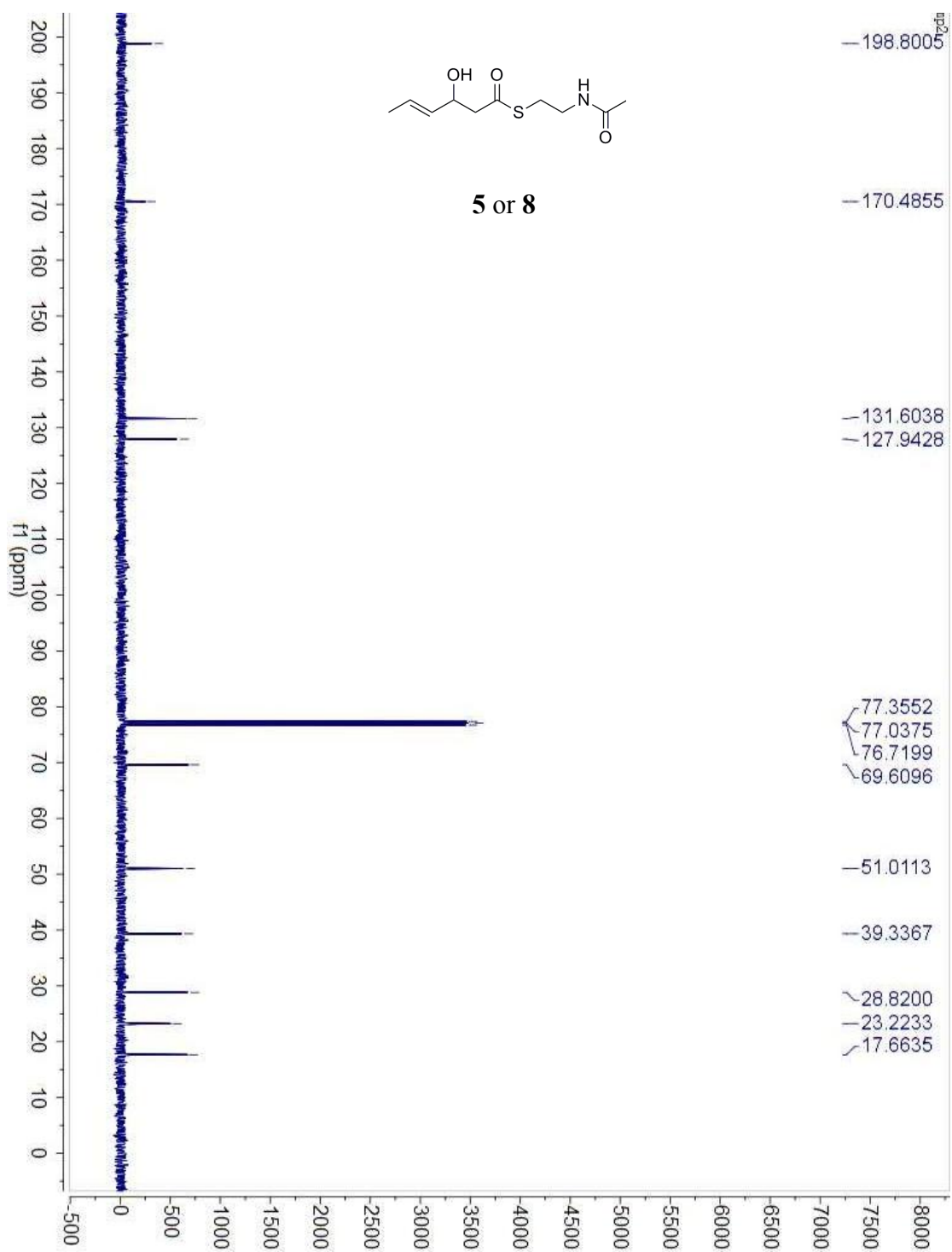


Figure S13. ^{13}C NMR (100 MHz) spectrum of compound **5** or **8** in CDCl_3

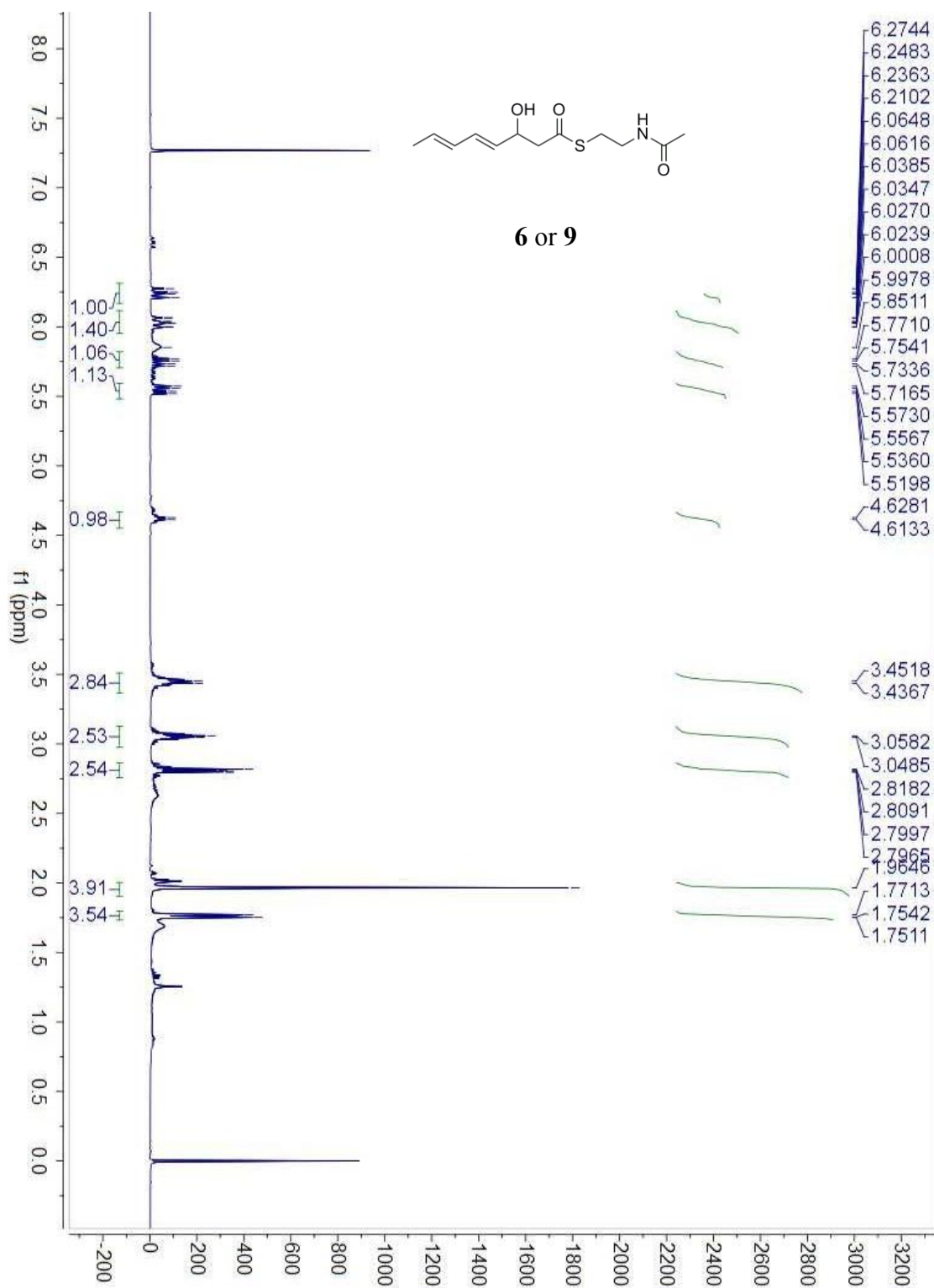


Figure S14. ^1H NMR (400 MHz) spectrum of compound **6** or **9** in CDCl_3

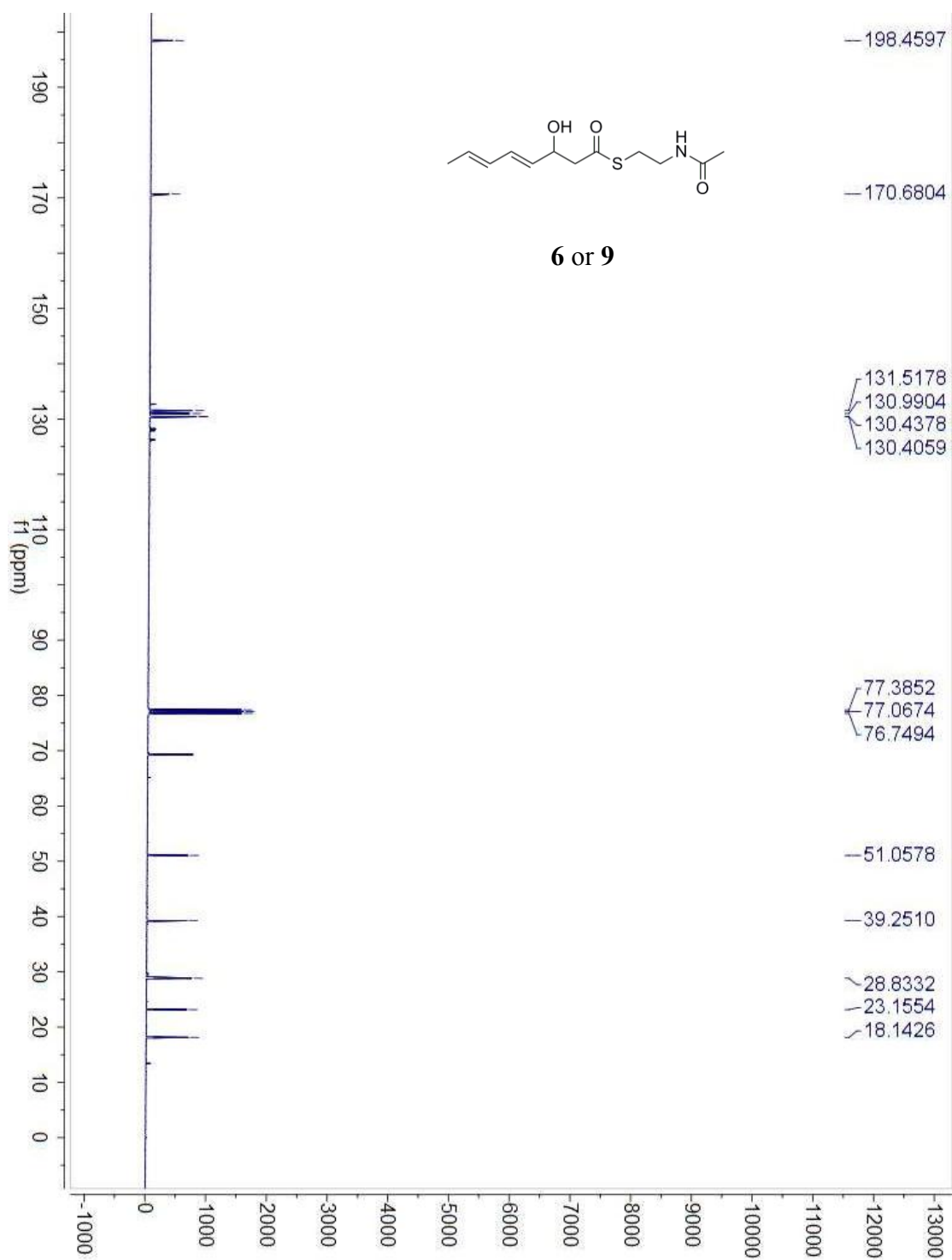


Figure S15. ^{13}C NMR (100 MHz) spectrum of compound **6 or 9** in CDCl_3

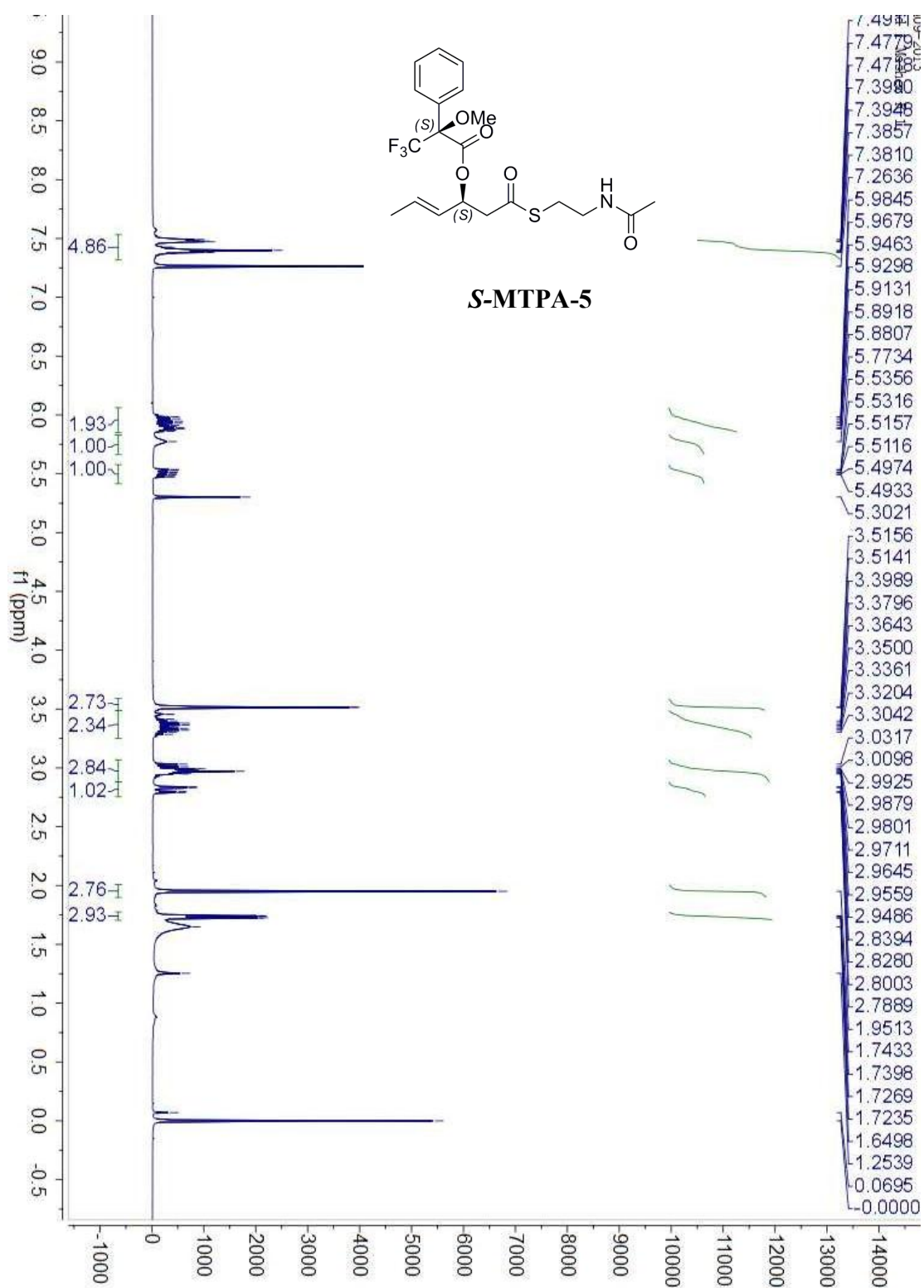


Figure S16. ^1H NMR (400 MHz) spectrum of compound *S*-MTPA-5 in CDCl_3

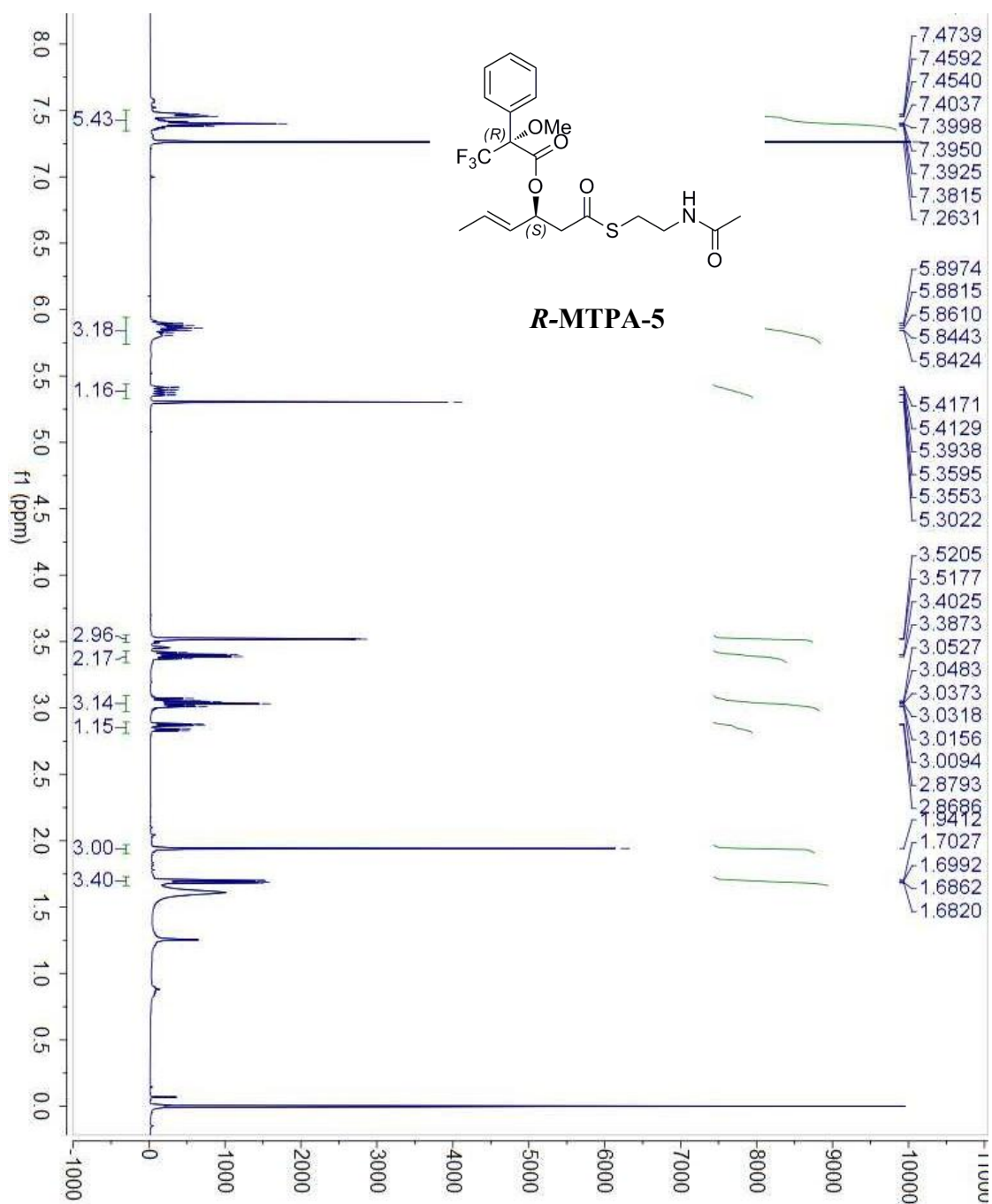


Figure S17. ¹H NMR (400 MHz) spectrum of compound *R*-MTPA-5 in CDCl₃

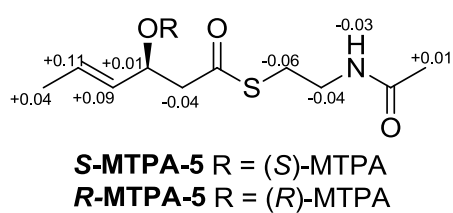


Figure S18. $\Delta\delta_{S-R}$ values (ppm) of MTPA esters for compound **5**.

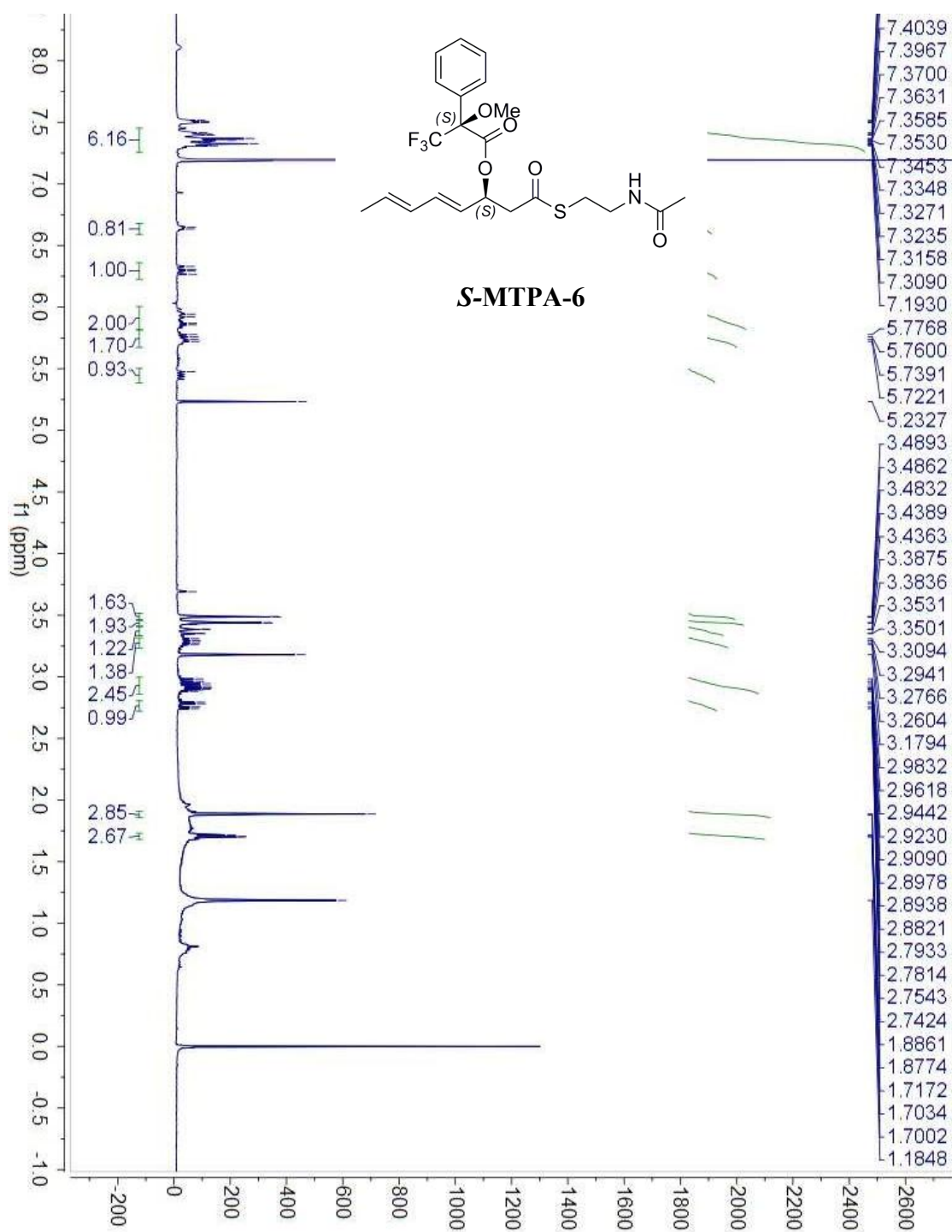


Figure S19. ^1H NMR (400 MHz) spectrum of compound *S*-MTPA-6 in CDCl_3

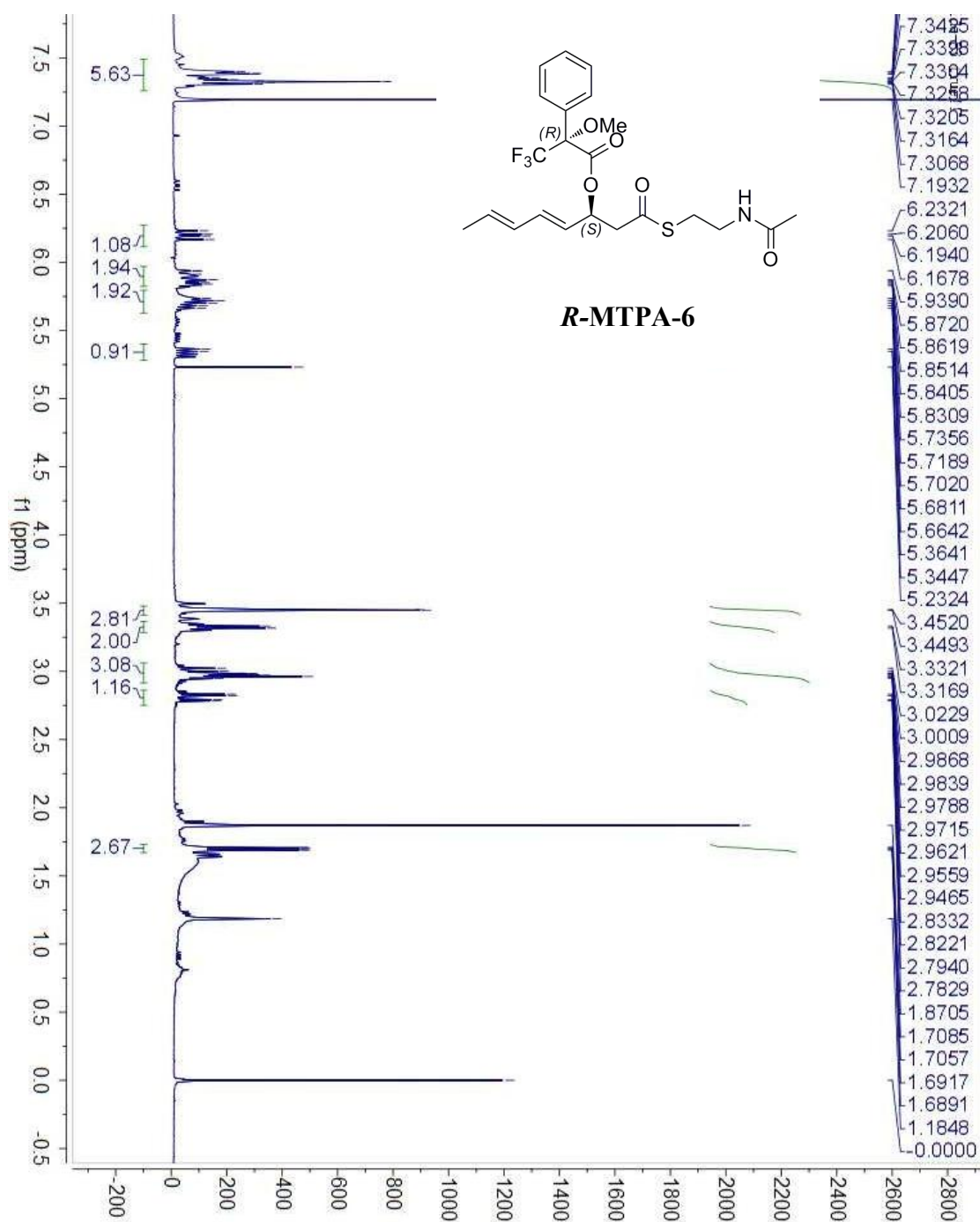


Figure S20. ^1H NMR (400 MHz) spectrum of compound *R*-MTPA-6 in CDCl_3

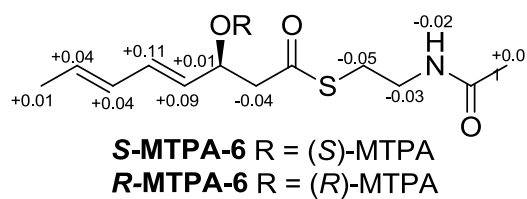


Figure S21. $\Delta\delta_{S-R}$ values (ppm) of MTPA esters for compound **6**.

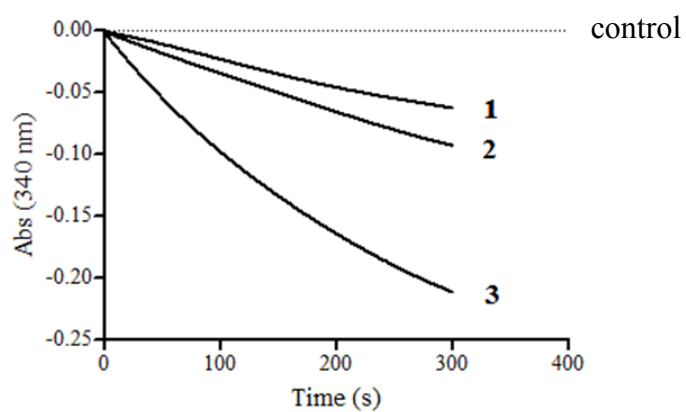


Figure S22. Enzymatic assays of PKSE-KRs by continuous photometric measurement at 340 nm to follow the time-dependent depletion of NADPH as exemplified by SgcE-KR with the three β -ketoacyl-SNAC substrates, **1**, **2**, and **3**.

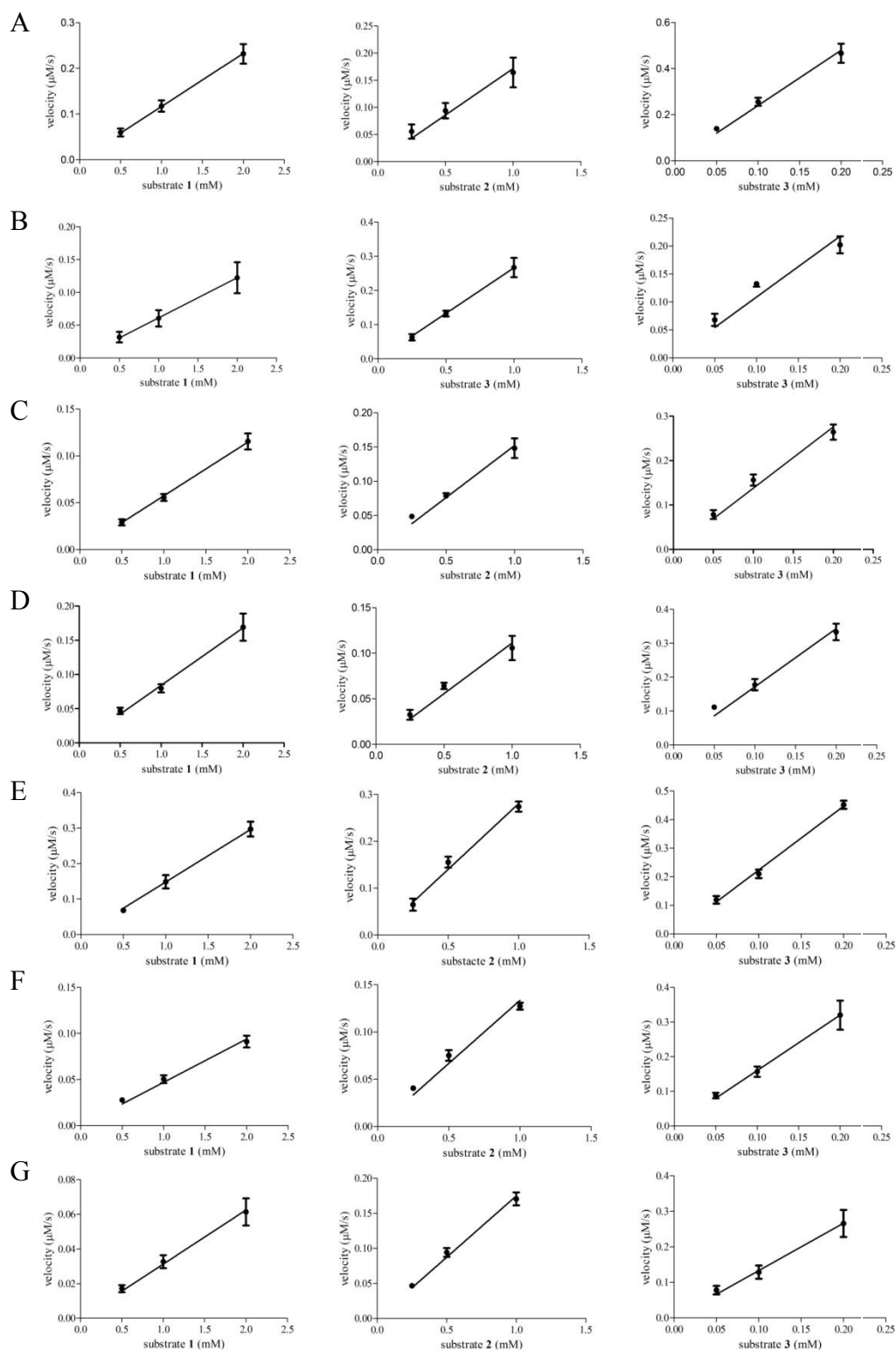


Figure S23. Pseudo-first order kinetic characterization of PKSE-KRs with the three β -ketoacyl-SNAC substrates, 1, 2, and 3: A, SgcE-KR; B, KedE-KR; C, MdpE-KR; D, NcsE-KR; E, CalE8-KR; F, DynE8-KR; G, UcmE-KR.